Broadband coherent multidimensional variational measurement

Sergey P. Vyatchanin,[1,2,*] Albert I. Nazmiev,[1] and Andrey B. Matsko[3]
[1]Faculty of Physics, M. V. Lomonosov Moscow State University, Leninskie Gory, Moscow 119991, Russia
[2]Quantum Technology Centre, M. V. Lomonosov Moscow State University, Leninskie Gory, Moscow 119991, Russia
[3]Jet Propulsion Laboratory, California Institute of Technology, 4800 Oak Grove Drive, Pasadena, California 91109-8099, USA

(Received 12 May 2022; revised 21 August 2022; accepted 31 October 2022; published 14 November 2022)

The standard quantum limit (SQL) of a classical mechanical force detection results from quantum back action perturbing evolution of a mechanical system. In this paper we show that usage of a multidimensional optical transducer may enable a broadband quantum back action evading measurement. We study theoretically a corresponding technique of measurement of a resonant signal force acting on a linear mechanical oscillator coupled to a generic optical system with three optical modes with separation nearly equal to the mechanical frequency. The measurement is performed by optical pumping of the central optical mode and analyzing the light escaping the two other modes. By detecting optimal quadrature components of the optical modes and postprocessing the measurement results we are able to exclude the back action in a broad frequency band and characterize the force with sensitivity better than the SQL. We show that the proposed scheme is similar to the multidimensional system containing quantum-mechanics-free subsystems which can evade the SQL using the idea of the so-called negative mass [M. Tsang and C. M. Caves, Phys. Rev. X **2**, 031016 (2012).].

DOI: 10.1103/PhysRevA.106.053711

I. INTRODUCTION

Mechanical motion is frequently tracked by usage of optical transducers. These transducers enable one to detect displacement, speed, acceleration, and rotation of mechanical systems. Mechanical motion can change frequency, amplitude, and phase of the probe light. The sensitivity of the measurement can be extremely high. For example, a relative mechanical displacement orders of magnitude smaller than a proton size can be detected. This feature is utilized in gravitational wave detectors [1–6], in magnetometers [7,8], and in torque sensors [9–11].

There are several reasons limiting the fundamental sensitivity of the measurement. One of them is the fundamental thermodynamic fluctuations of the probe mechanical system. The absolute position measurement is restricted due to the Nyquist noise. However, this obstacle can be either decreased or removed if one measures a variation of the position during time much faster than the system ring down time [12,13].

Another restriction comes from the quantum noise of the meter. On one hand, the accuracy of the measurements is limited because of their fundamental quantum fluctuations, represented by the shot noise for the optical probe wave. On the other hand, the sensitivity is impacted by the perturbation of the state of the probe mass due to the so-called back action. In the case of optical meter the mechanical perturbation results from fluctuations of the light pressure force. An interplay between these two phenomena leads to a so-called standard quantum limit (SQL) [12,13] of the sensitivity.

The reason for the SQL is the noncommutativity between the probe noise and the quantum back action noise. In a simple optical displacement sensor the probe noise is represented by the phase noise of the light and the back action noise stems from the amplitude noise of the light. The signal is contained in the phase of the probe. The relative phase noise decreases with optical power. The relative back action noise increases with the power. The optimal measurement sensitivity corresponds to the SQL. It is not possible to measure the amplitude noise and subtract it from the phase measurement result, because phase and amplitude quantum fluctuations of the same wave do not commute and, hence, do not correlate with each other.

The SQL of a mechanical force, acting on a free test mass, can be surpassed in a configuration supporting optomechanical velocity measurement [14,15]. The limit also can be overcome using an optomechanical rigidity [16,17]. Preparation of the probe light in a nonclassical state [18–24] as well as detection of a variation of a strongly perturbed optical quadrature [25–27] curb the quantum back action and lift the SQL. The SQL can be surpassed with coherent quantum noise cancellation [28–30] as well as compensation using an auxiliary medium with negative nonlinearity [31]. Optimization of the measurement scheme by usage of a few optical frequency harmonics as a probe also allows beating the SQL. A dichromatic optical probe may lead to observation of such phenomena as negative radiation pressure [32,33] and optical quadrature-dependent quantum back action evasion [34].

The first way of back action evading (BAE) for a mechanical oscillator, proposed about 40 years ago [35,36], took advantage of short (stroboscopic) measurements of a mechanical coordinate separated by a half period of the oscillator. At the same time it was proposed to measure not a coordinate but one of the quadrature amplitudes of a mechanical oscillator [35,37] to perform a BAE. Both propositions are equivalent and can be realized with a pulsing pump [36,38,39].

The measurement proposed here belongs to the class of broadband variational [27] measurements of a force acting

*svyatchanin@phys.msu.ru

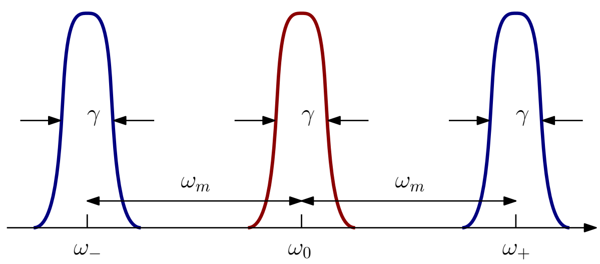

FIG. 1. A generic optomechanical configuration of the mechanical force detection. Three optical modes are involved in the interaction with the mechanical oscillator. The separation frequencies of the optical modes correspond to the frequency of the mechanical oscillator ω_m. Optical relaxation rate γ is the same for all three modes, $\gamma \ll \omega_m$. The middle mode characterized with frequency ω_0 is resonantly pumped with coherent light. The classical force of interest acts on the mechanical oscillator.

on a mechanical oscillator. Unlike the standard variational measurement technique, though, the method considered in this paper is optimized for the detection of the resonant mechanical force. The measurement strategy involves a coherent pump of the main optical mode at frequency ω_0 and optomechanical excitation of two additional optical modes at frequencies $\omega_\pm = \omega_0 \pm \omega_m$ detuned from the pumped mode by the eigenfrequency of the mechanical oscillator ω_m. We propose to detect the light escaping modes $\omega_\pm$ independently, measuring an optimal optical quadrature in each channel using balanced homodyne detection with carrier frequencies $\omega_\pm$. Such a two channel registration allows us to detect back action and remove it completely from the measured data.

It was shown recently that a multidimensional quantum system may have subsystems that behave classically [40]. All the observables of these quantum-mechanics-free subsystem (QMFS) can be used for quantum nondemolition (QND) measurements. The noncompatible variables are not coupled in one QMFS and the back action is caused by the observables from another QMFS and, hence, can be removed. We have studied the two-mode optomechanical readout and noticed that in some realizations of such a system the back action, defined by the sum of quadrature components $(a_+ + a_+^\dagger + a_- + a_-^\dagger)/2$ of the modes (here $a_\pm$ and $a_\pm^\dagger$ are the slow amplitudes of the annihilation and creation operators in optical modes $\pm$, detuned from the pump frequency by ω_m; see Fig. 1), impacts the difference of the quadrature components of the modes $(a_+ + a_+^\dagger - a_- - a_-^\dagger)/2$. These two linear combinations of the quadrature components do not commute and, hence, the measurement is not fundamentally limited by QND, in accordance with [40]. Importantly, to realize a BAE in the scheme one has to postprocess a linear combination of the measured quadratures with spectral frequency-dependent *complex* coefficients. This type of measurement can be performed if each of the spectral components is detected by a separate homodyne detector. The measurement result is multiplied on the optimal complex parameter, and the results are added together for the force determination.

The measurement idea is introduced in Sec. II using the idealized all-resonant physical model. The sensitivity of a system with frequency detunings is studied in Sec. III. It is shown that the nonequidistant modes deteriorate performance of the method. In Sec. IV we relate the proposed technique with the QND measurements involving the QMFS [40]. Possible realizations of the generic measurement technique are discussed in Sec. V. Section VI concludes the paper.

II. PHYSICAL MODEL

Let us consider three optical modes with frequencies ω_-, ω_0, and ω_+ separated by the eigenfrequency ω_m of the mechanical oscillator, as illustrated by Fig. 1. The middle mode characterized with frequency ω_0 is resonantly pumped, and the modes $\omega_\pm$ are not pumped. The mechanical oscillator is coupled with optical modes. The photons in the modes are generated due to parametric interaction of the optical pump and the mechanical signal photons. We detect output of the sideband modes $\omega_\pm$.

We assume that the relaxation rates of the optical modes are identical and characterized with the full width at half maximum equal to 2γ. The mechanical relaxation rate γ_m is small as compared with the optical one. We also assume that the conditions of the resolved sideband interaction and frequency synchronization are valid:

$$\gamma_m \ll \gamma \ll \omega_m, \quad \omega_0 - \omega_- = \omega_+ - \omega_0 = \omega_m. \tag{2.1}$$

At this stage we do not specify a physical realization of the measurement scheme and consider the outlined generic configuration. Two possible physical realizations of the measurement scheme are described in Sec. V.

A. Hamiltonian

The generalized Hamiltonian describing the system can be presented in the form

$$H = H_0 + H_{\rm int} + H_s + H_T + H_\gamma + H_{T,m} + H_{\gamma_m},$$
$$H_0 = \hbar\omega_+ \hat c_+^\dagger \hat c_+ + \hbar\omega_0 \hat c_0^\dagger \hat c_0 + \hbar\omega_- \hat c_-^\dagger \hat c_- + \hbar\omega_m \hat d^\dagger \hat d, \tag{2.2a}$$

$$H_{\rm int} = \frac{\hbar}{i}(\eta[\hat c_0^\dagger \hat c_- + \hat c_+^\dagger \hat c_0]\hat d - \eta^*[\hat c_0 \hat c_-^\dagger + \hat c_+ \hat c_0^\dagger]\hat d^\dagger), \tag{2.2b}$$

$$\hat H_s = -F_s x_0(\hat d + \hat d^\dagger). \tag{2.2c}$$

Here $\hat d$ and $\hat d^\dagger$ are annihilation and creation operators of the mechanical oscillator, and $\hat c_\pm$ and $\hat c_\pm^\dagger$ are annihilation and creation operators of the corresponding optical modes. The operator of coordinate x of the mechanical oscillator can be presented in the form

$$x = x_0(\hat d + \hat d^\dagger), \quad x_0 = \sqrt{\frac{\hbar}{2m\omega_m}}. \tag{2.3}$$

$H_{\rm int}$ is the Hamiltonian of the interaction between optical and mechanical modes. The interaction Hamiltonian is defined as $H_{\rm int} \sim (E_0 + E_+ + E_-)^2 x$, where E_0, E_-, and E_+ are the electric fields of modes 0, $-$, and $+$ on the surface of a mirror constituting the lump mass of the oscillator. These fields can be presented as $E_0 \equiv {\rm const} \times (\hat c_0 e^{-i\omega_0 t} + \hat c_0^\dagger e^{i\omega_0 t})$ and $E_\pm \equiv {\rm const} \times (\hat c_\pm e^{-i\omega_\pm t} + \hat c_\pm^\dagger e^{i\omega_\pm t})$. Then the interaction Hamiltonian can be transformed into the form of (2.2b) after omitting the fast oscillating terms. Parameter η stands for the coupling constant. H_s is a part of the Hamiltonian describing interaction of the mechanical oscillator with a classical signal force F_s. H_T is the Hamiltonian describing the environment (thermal bath) and H_γ is the Hamiltonian of the coupling between the environment and the optical modes, ultimately resulting in decay rate γ and the fluctuational forces acting on the system. We neglect the internal loss in the optical system and consider only the decay resulting from the unitary coupling of the modes with the external environment. The pump is also included into H_γ. Similarly, $H_{T,m}$ is the Hamiltonian of the environment and H_{γ_m} is the Hamiltonian describing coupling between the environment and the mechanical oscillator resulting in decay rate γ_m. See Appendix A for details.

We denote the normalized input and output optical amplitudes as $\hat{a}_{\pm,0}$ and $\hat{b}_{\pm,0}$, correspondingly. Using the Hamiltonian (2.2) we derive the Langevin equations of motion for the intracavity fields (see Appendix A for the full derivation). And introducing slow amplitudes in the conventional way

$$\hat{c}_0 \to \hat{c}_0 e^{-i\omega_0 t}, \quad \hat{c}_\pm \to \hat{c}_\pm e^{-i\omega_\pm t}, \quad \hat{d} \to \hat{d} e^{-i\omega_m t},$$

we finally obtain

$$\dot{\hat{c}}_0 + \gamma \hat{c}_0 = \eta^* \hat{c}_+ \hat{d}^\dagger - \eta \hat{c}_- \hat{d} + \sqrt{2\gamma}\, \hat{a}_0, \tag{2.4a}$$

$$\dot{\hat{c}}_- + \gamma \hat{c}_- = \eta^* \hat{c}_0 \hat{d}^\dagger + \sqrt{2\gamma}\, \hat{a}_-, \tag{2.4b}$$

$$\dot{\hat{c}}_+ + \gamma \hat{c}_+ = -\eta \hat{c}_0 \hat{d} + \sqrt{2\gamma}\, \hat{a}_+, \tag{2.4c}$$

$$\dot{\hat{d}} + \gamma_m \hat{d} = \eta^* (\hat{c}_0 \hat{c}_-^\dagger + \hat{c}_0^\dagger \hat{c}_+) + \sqrt{2\gamma_m}\, \hat{q} + f_s. \tag{2.4d}$$

Here $\hat{q}$ is the normalized fluctuation force acting on the mechanical oscillator, and f_s is the normalized signal force [see definition (2.20) below].

The input-output relations connecting the external and intracavity optical fields are

$$\hat{b}_\pm = -\hat{a}_\pm + \sqrt{2\gamma} \hat{c}_\pm. \tag{2.5}$$

It is convenient to separate the expectation values of the wave amplitudes at frequency ω_0 (described by block letters) as well as its fluctuation part (described by small letters) and assume that the fluctuations are small:

$$\hat{c}_0 = C_0 e^{-i\omega_0 t} + \tilde{c}_0 e^{-i\omega_0 t}. \tag{2.6}$$

C_0 stands for the expectation value of the field amplitude in the mode with eigenfrequency ω_0 and $\tilde{c}_0$ represents the quantum fluctuations of the field in the mode, $|C_0|^2 \gg \langle \tilde{c}_0^\dagger \tilde{c}_0 \rangle$, where $\langle \dots \rangle$ stands for ensemble averaging. Similar expressions can be written for the optical modes with eigenfrequencies $\omega_\pm$ and the mechanical mode with eigenfrequency ω_m. The normalization of the amplitudes is selected so that $\hbar\omega_0 |A_0|^2$ describes the optical power [27], whereas $\hbar\omega_0 |C_0|^2$ describes optical energy in the cavity.

Using the equations of motion (2.4) and assuming that $A_+ = A_- = 0$ (the regular signal contribution is considered in the fluctuational parts) we get the (zeroth order of approximation) equations for the expectation values:

$$\gamma C_0 = \eta^* C_+ D^* - \eta C_- D + \sqrt{2\gamma} A_0, \tag{2.7a}$$

$$\gamma C_- = \eta^* C_0 D^*, \tag{2.7b}$$

$$\gamma C_+ = -\eta C_0 D, \tag{2.7c}$$

$$\gamma_m D = \eta^* (C C_-^* + C^* C_+). \tag{2.7d}$$

This set of equations has an obvious stationary solution:

$$C_0 = \sqrt{\frac{2}{\gamma}} A_0, \quad C_- = C_+ = 0, \quad D = 0. \tag{2.8}$$

Substituting Eq. (2.8) into the equations of motion (2.4) we derive the stability conditions for this solution:

$$\dot{\tilde{c}}_0 + \gamma \tilde{c}_0 = 0, \tag{2.9a}$$

$$\dot{\hat{c}}_- + \gamma \hat{c}_- = \eta^* C_0 \hat{d}^*, \tag{2.9b}$$

$$\dot{\hat{c}}_+ + \gamma \hat{c}_+ = -\eta C_0 \hat{d}, \tag{2.9c}$$

$$\dot{\hat{d}} + \gamma_m \hat{d} = \eta^* (\hat{c}_-^* C_0 + \hat{c}_+ C_0^*). \tag{2.9d}$$

The first equation (2.9a) for the middle mode separates from the other three.

Substituting $\hat{c}_+ = c_+ e^{\lambda t}$, $\hat{c}_- = c_- e^{\lambda t}$, and $\hat{d} = d e^{\lambda t}$ we get

$$\begin{aligned} (\lambda + \gamma) c_-^* + 0 c_+ - \eta C_0^* d &= 0, \\ 0 c_-^* + (\lambda + \gamma) c_+ + \eta C_0 d &= 0, \\ -\eta^* C_0 c_-^* - \eta^* C_0^* c_+ - (\lambda + \gamma_m) d &= 0. \end{aligned} \tag{2.10}$$

We utilize the equation conjugated to (2.9b) in order to exclude d^*. It allows creating a complete set of equations. Solving equation $\Delta = 0$, where Δ is the determinant of this set of linear equations, we obtain $\lambda_{1,2} = -\gamma < 0$ and $\lambda_3 = -\gamma_m < 0$, hence the solution of the linearized equations (2.8) is stable.

Substituting the solution (2.8) into the equations of motion (2.4) we finally obtain

$$\dot{\tilde{c}}_0 + \gamma \tilde{c}_0 = \sqrt{2\gamma} \hat{a}_0, \tag{2.11a}$$

$$\dot{\hat{c}}_+ + \gamma \hat{c}_+ + \eta C_0 \hat{d} = \sqrt{2\gamma} \hat{a}_+, \tag{2.11b}$$

$$\dot{\hat{c}}_- + \gamma \hat{c}_- - \eta^* C_0^* \hat{d}^\dagger = \sqrt{2\gamma} \hat{a}_-, \tag{2.11c}$$

$$\dot{\hat{d}} + \gamma_m \hat{d} - \eta^* [C_0 \hat{c}_-^\dagger + \hat{c}_+ C_0^*] = \sqrt{2\gamma_m} \hat{q} + f_s. \tag{2.11d}$$

Spectra of outputs $b_\pm$ (2.5) localized around frequencies $\omega_\pm$ have to be detected separately, as shown in Fig. 2. We also see that fluctuation waves around ω_0 do not influence field components in the vicinity of frequencies $\omega_\pm$ and the first equation (2.11a) separates from the other three, so it is omitted from further consideration.

We assume in what follows that the expectation amplitudes are real, the same as the coupling constant η:

$$C_0 = C_0^*, \quad A_0 = A_0^*, \quad \eta = \eta^*. \tag{2.12}$$

The operators $\hat{a}_\pm$ are characterized with the following commutators and correlators:

$$[\hat{a}_\pm(t), \hat{a}_\pm^\dagger(t')] = \delta(t - t'), \tag{2.13}$$

$$\langle \hat{a}_\pm(t) \hat{a}_\pm^\dagger(t') \rangle = \delta(t - t'), \tag{2.14}$$

where $\langle \dots \rangle$ stands for ensemble averaging. This is true since the incident fields are considered to be in the coherent state.

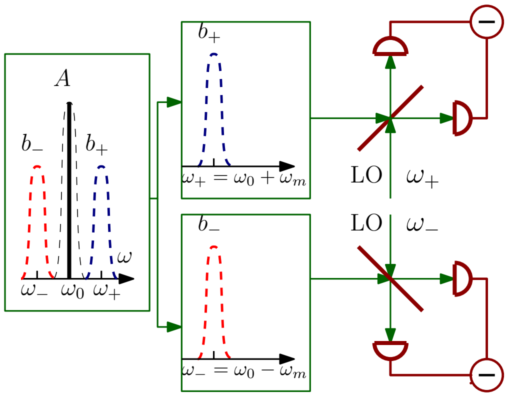

FIG. 2. A schematic explaining the basic principle of the measurement. Quadrature components of the output modes $b_\pm$ are measured separately by balanced homodyne detectors with corresponding optimal local oscillators having frequencies $\omega_\pm$. The signal is inferred by processing of the linear combination of the measured results. Essentially, the linear combination in the frequency domain should have complex frequency dependent coefficients.

The Fourier transform of these operators is defined as follows:

$$\hat{a}_\pm(t) = \int_{-\infty}^{\infty} a_\pm(\Omega)\, e^{-i\Omega t}\, \frac{d\Omega}{2\pi}. \tag{2.15}$$

Similar expressions can be written for the other operators. Using (2.13) and (2.14) we derive commutators and correlators for the Fourier amplitudes of the input fluctuation operators:

$$[a_\pm(\Omega), a_\pm^\dagger(\Omega')] = 2\pi\, \delta(\Omega - \Omega'), \tag{2.16}$$

$$\langle a_\pm(\Omega) a_\pm^\dagger(\Omega')\rangle = 2\pi\, \delta(\Omega - \Omega'). \tag{2.17}$$

B. Solution

The Fourier amplitudes for the the intracavity field as well as mechanical amplitude, $c_\pm$ and d, can be found utilizing (2.11b) and (2.11c):

$$\begin{aligned}
&(\gamma - i\Omega)c_+(\Omega) + \eta C_0 d(\Omega)\\
&\quad = \sqrt{2\gamma}\, a_+(\Omega), &(2.18a)\\
&(\gamma - i\Omega)c_-(\Omega) - \eta C_0 d^\dagger(-\Omega)\\
&\quad = \sqrt{2\gamma}\, a_-(\Omega), &(2.18b)\\
&(\gamma_m - i\Omega)d(\Omega) - \eta C_0[c_+(\Omega) + c_-^\dagger(-\Omega)]\\
&\quad = \sqrt{2\gamma_m}\, q(\Omega) + f_s(\Omega), &(2.18c)\\
&b_\pm(\Omega)\\
&\quad = -a_\pm(\Omega) + \sqrt{2\gamma}\, c_\pm(\Omega). &(2.18d)
\end{aligned}$$

We assume that the signal force is a resonant square pulse acting during time interval τ:

$$\begin{aligned}
F_S(t) &= F_{s0}\sin(\omega_m t + \psi_f)\\
&= i(F_s(t)e^{-i\omega_m t} - F_s^*(t)e^{i\omega_m t}), \quad -\frac{\tau}{2} < t < \frac{\tau}{2},
\end{aligned} \tag{2.19}$$

$$f_s(\Omega) = \frac{F_s(\Omega)}{\sqrt{2\hbar\omega_m m}}, \quad f_{s0}(\Omega) = \frac{F_{s0}(\Omega)}{\sqrt{2\hbar\omega_m m}} = 2 f_s(\Omega) \tag{2.20}$$

where $F_s(\Omega) \neq F_s^*(-\Omega)$ is the Fourier amplitude of $F_s(t)$.

The Fourier amplitudes of the thermal noise operators $\hat{q}$ obey the relations

$$[q(\Omega),\, q^\dagger(\Omega')] = 2\pi\, \delta(\Omega - \Omega'), \tag{2.21a}$$
$$\langle q(\Omega)\, q^\dagger(\Omega')\rangle = 2\pi\, (2n_T + 1)\, \delta(\Omega - \Omega'), \tag{2.21b}$$
$$n_T = \frac{1}{e^{\hbar\omega_m/\kappa_B T} - 1}, \tag{2.21c}$$

where κ_B is the Boltzmann constant and T is the ambient temperature.

Introducing quadrature amplitudes of amplitude and phase

$$a_{\pm a} = \frac{a_\pm(\Omega) + a_\pm^\dagger(-\Omega)}{\sqrt{2}}, \tag{2.22a}$$

$$a_{\pm\phi} = \frac{a_\pm(\Omega) - a_\pm^\dagger(-\Omega)}{i\sqrt{2}} \tag{2.22b}$$

(the quadrature amplitudes for the other operators are introduced in the same way) and using (2.18) we obtain

$$(\gamma - i\Omega)c_{+a} + \eta C_0 d_a = \sqrt{2\gamma}\, a_{+a}, \tag{2.23a}$$
$$(\gamma - i\Omega)c_{+\phi} + \eta C_0 d_\phi = \sqrt{2\gamma}\, a_{+\phi}, \tag{2.23b}$$
$$(\gamma - i\Omega)c_{-a} - \eta C_0 d_a = \sqrt{2\gamma}\, a_{-a}, \tag{2.23c}$$
$$(\gamma - i\Omega)c_{-\phi} + \eta C_0 d_\phi = \sqrt{2\gamma}\, a_{-\phi}, \tag{2.23d}$$
$$(\gamma_m - i\Omega)d_a - \eta C_0(c_{+a} + c_{-a}) = \sqrt{2\gamma_m} q_a + f_{s\,a}, \tag{2.23e}$$
$$(\gamma_m - i\Omega)d_\phi - \eta C_0(c_{+\phi} - c_{-\phi}) = \sqrt{2\gamma_m} q_\phi + f_{s\,\phi}. \tag{2.23f}$$

Please note that sum $c_{+a} + c_{-a}$ does not contain information on the mechanical motion (the term proportional to $\sim d_a$ is absent), but produces the back action term in (2.23e). Introducing sums and differences of the quadratures

$$g_{a\pm} = \frac{c_{+a} \pm c_{-a}}{\sqrt{2}}, \quad g_{\phi\pm} = \frac{c_{+\phi} \pm c_{-\phi}}{\sqrt{2}}, \tag{2.24}$$
$$\alpha_{a\pm} = \frac{a_{+a} \pm a_{-a}}{\sqrt{2}}, \quad \alpha_{\phi\pm} = \frac{a_{+\phi} \pm a_{-\phi}}{\sqrt{2}}, \tag{2.25}$$
$$\beta_{a\pm} = \frac{b_{+a} \pm b_{-a}}{\sqrt{2}}, \quad \beta_{\phi\pm} = \frac{b_{+\phi} \pm b_{-\phi}}{\sqrt{2}} \tag{2.26}$$

and rewriting (2.23) in the new notations we obtain

$$(\gamma - i\Omega)g_{a+} = \sqrt{2\gamma}\alpha_{a+}, \tag{2.27a}$$
$$(\gamma - i\Omega)g_{a-} + \sqrt{2}\eta C_0 d_a = \sqrt{2\gamma}\alpha_{a-}, \tag{2.27b}$$
$$(\gamma_m - i\Omega)d_a - \sqrt{2}\eta C_0 g_{a+} = \sqrt{2\gamma_m} q_a + f_{s\,a}, \tag{2.27c}$$
$$(\gamma - i\Omega)g_{\phi+} + \sqrt{2}\eta C_0 d_\phi = \sqrt{2\gamma}\alpha_{\phi+}, \tag{2.27d}$$
$$(\gamma - i\Omega)g_{\phi-} = \sqrt{2\gamma}\alpha_{\phi-}, \tag{2.27e}$$
$$(\gamma_m - i\Omega)d_\phi - \sqrt{2}\eta C_0 g_{\phi-} = \sqrt{2\gamma_m} q_\phi + f_{s\,\phi}. \tag{2.27f}$$

The sets (2.27a)–(2.27c) and (2.27d)–(2.27f) can be separated.

It is convenient to present the solution of the set (2.27a)–(2.27c) for the amplitude quadratures in the form

$$\beta_{a+} = \xi\, \alpha_{a+}, \quad \xi = \frac{\gamma + i\Omega}{\gamma - i\Omega}, \tag{2.28a}$$

$$\beta_{a-} = \xi \left(\alpha_{a-} - \frac{\mathcal{K}\, \alpha_{a+}}{\gamma_m - i\Omega} \right) \tag{2.28b}$$

$$- \frac{\sqrt{\xi \mathcal{K}}}{\gamma_m - i\Omega} (\sqrt{2\gamma_m} q_a + f_{s\,a}), \tag{2.28c}$$

$$\mathcal{K} \equiv \frac{4\gamma\, \eta^2 C_0^2}{\gamma^2 + \Omega^2}. \tag{2.28d}$$

As expected, the back action term is proportional to the normalized probe power $\mathcal{K}$ in Eq. (2.28b). However, this term can be excluded by the postprocessing. One can measure *both* β_{+a} and β_{-a} simultaneously and subtract β_{+a} from β_{-a} to remove the back action completely. It means that we can measure combination

$$\beta_{a-}^{\rm comb} = \beta_{a-} + \frac{\mathcal{K}\, \beta_{a+}}{\gamma_m - i\Omega} \tag{2.29}$$

$$= \quad \xi \alpha_{a-} - \frac{\sqrt{\xi \mathcal{K}}}{\gamma_m - i\Omega} (\sqrt{2\gamma_m} q_a + f_{s\,a}), \tag{2.30}$$

which is back action free. This is one of the main findings of the paper. Essentially, the coefficient needed for suppression of the back action is complex. It depends on the spectral frequency Ω. While a similar result was obtained earlier [34], the measurement scheme considered here involves a single probe beam and is stable. It does not use the dichromatic pump introducing resonant mechanical motion that has to be controlled.

Let us analyze the measurement sensitivity. We find the force detection condition using single-sided power spectral density $S_f(\Omega)$ for signal force (2.19). Assuming that the detection limit corresponds to the signal-to-noise ratio exceeding unity, we recalculate (2.28b) as

$$\frac{\beta_{a-}(\gamma_m - i\Omega)}{\sqrt{\xi \mathcal{K}}} = -f_{s0} - \sqrt{2\gamma_m}\, q_a \tag{2.31a}$$

$$+ \frac{\sqrt{\xi}\, (\gamma_m - i\Omega)\, \alpha_{a-}}{\sqrt{\mathcal{K}}} - \alpha_{a+} \sqrt{\xi \mathcal{K}}, \tag{2.31b}$$

$$f_{s0} \geqslant \sqrt{S_f(\Omega) \frac{\Delta\Omega}{2\pi}}, \tag{2.31c}$$

where $\Delta\Omega \simeq 2\pi/\tau$, and use the right-hand side of the equation to find the spectral density of the force f_{s0} and demand its spectral density to exceed the spectral density of the noise terms q_a, α_{a-}, and α_{a+}.

Using (2.17) and (2.21b) we derive for the case when we measure β_{a-} (2.31)

$$S_f(\Omega) = 2\gamma_m(2n_T + 1) + \frac{\gamma_m^2 + \Omega^2}{\mathcal{K}} + \mathcal{K} \tag{2.32}$$

$$\geqslant 2\gamma_m(2n_T + 1) + S_{{\rm SQL},f}, \tag{2.33}$$

$$S_{{\rm SQL},f} = 2\sqrt{\gamma_m^2 + \Omega^2}. \tag{2.34}$$

The sensitivity is restricted by the SQL. If we measure $\beta_{a-}^{\rm comb}$ (2.30) the spectral density is not limited by the SQL:

$$S_f(\Omega) = 2\gamma_m(2n_T + 1) + \frac{\gamma_m^2 + \Omega^2}{\mathcal{K}}. \tag{2.35}$$

Here the first term describes thermal noise and the second one stands for the quantum measurement noise (shot noise) decreasing with the power increase. The back action term is excluded completely.

The thermal noise masks signals in any optomechanical detection scheme. It cannot be separated from the signal if it comes in the same channel as the force, at the same time, and with spectral components overlapping with the signal. The error associated with the thermal noise can exceed the measurement error related to the measurement system. A proper measurement procedure allows us to reduce the impact of the thermal noise not identical to the signal force and coming from the apparatus itself and also exclude the quantum uncertainty associated with the initial state of the mechanical system. The main requirement for such a measurement is fast interrogation time τ, which should be much shorter than the ring down time of the mechanical system, i.e., $\gamma_m \tau \ll 1$ [12,13]. This is possible if the measurement bandwidth exceeds the bandwidth of the mechanical mode. Sensitivity of narrowband resonant measurements is usually limited by the thermal noise.

One can measure sum and differences of the phase quadratures instead of the amplitude quadratures. Solving set (2.27d)–(2.27f) we arrive at

$$\beta_{\phi-} = \xi\, \alpha_{\phi-}, \tag{2.36a}$$

$$\beta_{\phi+} = \xi \left(\alpha_{\phi+} - \frac{\mathcal{K}\, \alpha_{\phi-}}{\gamma_m - i\Omega} \right) \tag{2.36b}$$

$$- \frac{\sqrt{\xi \mathcal{K}}}{\gamma_m - i\Omega} (\sqrt{2\gamma_m} q_\phi + f_{s\,\phi}). \tag{2.36c}$$

We can measure quadratures $\beta_{\pm\phi}$ simultaneously and subtract back action taking combination [compare with (2.29)]

$$\beta_{\phi+}^{\rm comb} = \beta_{\phi+} + \frac{\mathcal{K} \beta_{\phi-}}{\gamma_m - i\Omega}. \tag{2.36d}$$

A generalization is possible for a pair of quadrature components with arbitrary parameter φ:

$$b_{+\varphi} = b_{+a} \cos\varphi + b_{+\phi} \sin\varphi, \tag{2.37a}$$

$$b_{-\varphi} = b_{-a} \cos\varphi - b_{-\phi} \sin\varphi. \tag{2.37b}$$

The sum $b_{+\varphi} + b_{-\varphi}$ is not disturbed by the mechanical motion but contains the term proportional to the back action force, whereas the difference $b_{+\varphi} - b_{-\varphi}$ contains the term proportional to mechanical motion (with back action and signal). The back action term can be measured and subtracted from the force measurement result.

III. INFLUENCE OF THE DETUNING

Analysis in Sec. II B was made under the assumption that the difference between the frequencies of the consecutive optical modes is precisely equal to the mechanical frequency.

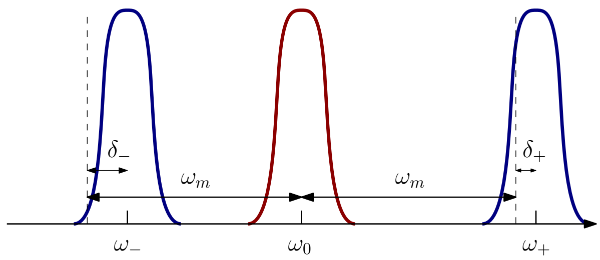

FIG. 3. General case of a nonequidistant triplet of optical modes.

In this section we analyze the system characterized with imperfect frequency synchronization conditions. Let us consider frequencies of the optical modes to be shifted by the arbitrary values δ_- for the left sideband and δ_+ for the right as shown in Fig. 3:

$$\omega - \omega_- = \omega_m - \delta_-, \quad \omega_+ - \omega = \omega_m + \delta_+. \tag{3.1}$$

The nonzero frequency detuning δ_0 of the pump light from the resonant frequency ω_0 and frequency detuning δ_f of the signal force from the mechanical frequency ω_m can be neglected here. The pump frequency can be locked to the resonator mode. We also expect that the dimensions of the optical resonator can be adjusted so that $\delta_f = 0$.

The simplified Langevin equations of motion take the following form:

$$\dot{\hat{c}}_0 + \gamma\hat{c}_0 = \eta^*\hat{c}_+\hat{d}^\dagger - \eta\hat{c}_-\hat{d} + \sqrt{2\gamma}\hat{a}_0, \tag{3.2a}$$

$$\dot{\hat{c}}_- + (\gamma - i\delta_-)\hat{c}_- = \eta^*\hat{c}_0\hat{d}^\dagger + \sqrt{2\gamma}\hat{a}_-, \tag{3.2b}$$

$$\dot{\hat{c}}_+ + (\gamma - i\delta_+)\hat{c}_+ = -\eta\hat{c}_0\hat{d} + \sqrt{2\gamma}\hat{a}_+, \tag{3.2c}$$

$$\dot{\hat{d}} + \gamma_m\hat{d} = \eta^*(\hat{c}_0\hat{c}_-^\dagger + \hat{c}_0^\dagger\hat{c}_+) + \sqrt{2\gamma_m}\hat{q} + f_s. \tag{3.2d}$$

The detuning values are considered to be small in comparison with the spectral width of the optical modes $\delta_\pm \ll \gamma$. The difference between (2.4) and (3.2) is in the presence of $i\delta_\pm\hat{c}_\pm$ terms in (3.2b) and (3.2c).

The expectation values for the amplitudes of the optical and mechanical modes are

$$C_0 = \sqrt{\frac{2}{\gamma}}A_0, \quad C_- = C_+ = D = 0. \tag{3.3}$$

The solution is stable as the roots of the characteristic equation are real and negative: $\mathrm{Re}\lambda_{1,2} = -\gamma < 0$, $\lambda_3 = -\gamma_m$.

For the sake of simplicity and consistency we assume that coupling constant η and the mean amplitude C_0 of the intracavity field are real:

$$C_0 = C_0^*, \quad \eta = \eta^*. \tag{3.4}$$

Substituting the expectation values of the amplitudes into (3.2) we derive the equations of motion for the Fourier amplitudes of the fluctuation parts of the optical sidebands and the the mechanical oscillation:

$$(\gamma - i\delta_- - i\Omega)c_- = \eta C_0 d^\dagger + \sqrt{2\gamma}a_-, \tag{3.5a}$$

$$(\gamma - i\delta_+ - i\Omega)c_+ = -\eta C_0 d + \sqrt{2\gamma}a_+, \tag{3.5b}$$

$$(\gamma_m - i\Omega)d = \eta C_0(c_-^\dagger + c_+) + \sqrt{2\gamma_m}q + f_s. \tag{3.5c}$$

Introducing the quadratures in the same way as we did it in (2.22), we obtain equations for the quadratures. We denote them with prime symbols to distinguish from (2.23):

$$c'_{+a} = \frac{(-\eta C_0 d_a + \sqrt{2\gamma}a_{+a})(\gamma - i\Omega)}{(\gamma - i\Omega)^2 + \delta_+^2} - \frac{\delta_+(-\eta C_0 d_\phi + \sqrt{2\gamma}a_{+\phi})}{(\gamma - i\Omega)^2 + \delta_+^2}, \tag{3.6a}$$

$$c'_{-a} = \frac{(\eta C_0 d_a + \sqrt{2\gamma}a_{-a})(\gamma - i\Omega)}{(\gamma - i\Omega)^2 + \delta_-^2} - \frac{\delta_-(-\eta C_0 d_\phi + \sqrt{2\gamma}a_{-\phi})}{(\gamma - i\Omega)^2 + \delta_-^2}, \tag{3.6b}$$

$$c'_{+\phi} = \frac{(-\eta C_0 d_\phi + \sqrt{2\gamma}a_{+\phi})(\gamma - i\Omega)}{(\gamma - i\Omega)^2 + \delta_+^2} + \frac{\delta_+(-\eta C_0 d_a + \sqrt{2\gamma}a_{+a})}{(\gamma - i\Omega)^2 + \delta_+^2}, \tag{3.6c}$$

$$c'_{-\phi} = \frac{(-\eta C_0 d_\phi + \sqrt{2\gamma}a_{-\phi})(\gamma - i\Omega)}{(\gamma - i\Omega)^2 + \delta_-^2} + \frac{\delta_-(\eta C_0 d_a + \sqrt{2\gamma}a_{-a})}{(\gamma - i\Omega)^2 + \delta_-^2}, \tag{3.6d}$$

$$(\gamma_m - i\Omega)d_a - \eta C_0(c_{+a} + c_{-a}) = \sqrt{2\gamma_m}q_a + f_{sa}, \tag{3.6e}$$

$$(\gamma_m - i\Omega)d_\phi - \eta C_0(c_{+\phi} - c_{-\phi}) = \sqrt{2\gamma_m}q_\phi + f_{s\phi}. \tag{3.6f}$$

The "new" quadratures (3.6) can be expressed as the linear combinations of "old" quadratures. Saving only terms linear over detuning values $\delta_\pm$ in (3.6) we obtain

$$c'_{+a} = c_{+a} - \frac{\delta_+}{\gamma - i\Omega}c_{+\phi}, \tag{3.7a}$$

$$c'_{-a} = c_{-a} - \frac{\delta_-}{\gamma - i\Omega}c_{-\phi}, \tag{3.7b}$$

$$c'_{+\phi} = c_{+\phi} + \frac{\delta_+}{\gamma - i\Omega}c_{+a}, \tag{3.7c}$$

$$c'_{-\phi} = c_{-\phi} + \frac{\delta_-}{\gamma - i\Omega}c_{-a}, \tag{3.7d}$$

$$(\gamma_m - i\Omega)d_a - \eta C_0(c_{+a} + c_{-a}) = \sqrt{2\gamma_m}q_a + f_{sa}, \tag{3.7e}$$

$$(\gamma_m - i\Omega)d_\phi - \eta C_0(c_{+\phi} - c_{-\phi}) = \sqrt{2\gamma_m}q_\phi + f_{s\phi}. \tag{3.7f}$$

We introduce the sum and difference of the quadratures as in (2.24) and save the terms proportional to the first order of $\delta_\pm$. It is also convenient to introduce symmetric and antisymmetric combinations of the detunings:

$$\Delta = \frac{\delta_+ + \delta_-}{2}, \qquad \delta = \frac{\delta_+ - \delta_-}{2}. \tag{3.8}$$

We denote the sum and the difference of the new quadratures by the prime symbols, and we express them as the linear combinations of the old (2.24) expressions:

$$g'_{a+} = g_{a+} - \frac{\delta}{\gamma - i\Omega} g_{\phi-} - \frac{\Delta}{\gamma - i\Omega} g_{\phi+}, \tag{3.9a}$$

$$g'_{a-} = g_{a-} - \frac{\Delta}{\gamma - i\Omega} g_{\phi-} - \frac{\delta}{\gamma - i\Omega} g_{\phi+}, \tag{3.9b}$$

$$(\gamma_m - i\Omega) d_a = \sqrt{2}\eta C_0 g_{a+} + \sqrt{2\gamma_m} q_a + f_a, \tag{3.9c}$$

$$g'_{\phi-} = g_{\phi-} + \frac{\delta}{\gamma - i\Omega} g_{a+} + \frac{\Delta}{\gamma - i\Omega} g_{a-}, \tag{3.9d}$$

$$g'_{\phi+} = g_{\phi+} + \frac{\Delta}{\gamma - i\Omega} g_{a+} + \frac{\delta}{\gamma - i\Omega} g_{a-}, \tag{3.9e}$$

$$(\gamma_m - i\Omega) d_\phi = \sqrt{2}\eta C_0 g_{\phi-} + \sqrt{2\gamma_m} q_\phi + f_\phi. \tag{3.9f}$$

The sum and difference of the amplitude quadratures of the output fields can be obtained using the input-output relations (2.5):

$$\beta'_{a+} = \beta_{a+} - \frac{\delta\sqrt{2\gamma}}{\gamma - i\Omega} g_{\phi-} - \frac{\Delta\sqrt{2\gamma}}{\gamma - i\Omega} g_{\phi+}, \tag{3.10a}$$

$$\beta'_{a-} = \beta_{a-} - \frac{\Delta\sqrt{2\gamma}}{\gamma - i\Omega} g_{\phi-} - \frac{\delta\sqrt{2\gamma}}{\gamma - i\Omega} g_{\phi+}. \tag{3.10b}$$

The measurement of the combination of the quadratures similar to (2.30) suppresses the major part of the back action, the same as in the perfectly tuned case. However, the parts proportional to δ and Δ cannot be removed:

$$\beta_a^{\text{comb}\prime} = \frac{\mathcal{K}}{\gamma_m - i\Omega} \beta'_{+a} + \beta'_{-a} \tag{3.11a}$$

$$\begin{aligned} &\approx \xi\alpha_{-a} - \frac{\sqrt{\xi\mathcal{K}}}{\gamma_m - i\Omega}(\sqrt{2\gamma_m} q_a + f_{sa}) \\ &- \frac{\mathcal{K}}{(\gamma_m - i\Omega)(\gamma - i\Omega)}\left[\delta - \frac{\Delta\xi\mathcal{K}}{(\gamma_m - i\Omega)}\right]\alpha_\phi \\ &- \frac{2\gamma\Delta\mathcal{K}}{(\gamma - i\Omega)^2(\gamma_m - i\Omega)}\alpha_{\phi+} \\ &+ \frac{\sqrt{\xi\mathcal{K}}\Delta\mathcal{K}}{(\gamma - i\Omega)(\gamma_m - i\Omega)^2}(\sqrt{2\gamma_m} q_\phi + f_{s\phi}). \end{aligned} \tag{3.11b}$$

In this case it is optimal to measure a combination of the quadrature components of the force:

$$f_s = \frac{f_{s,a} + D\mathcal{K} f_{s,\phi}}{\sqrt{1 + |D\mathcal{K}|^2}}, \tag{3.12}$$

where

$$D = \frac{\Delta}{(\gamma - i\Omega)(\gamma_m - i\Omega)}. \tag{3.13}$$

The noise power spectral density calculated from (3.11) takes the form

$$\begin{aligned} S(\Omega) &= 2\gamma_m(n_T + 1) + \frac{\gamma_m^2 + \Omega^2}{\mathcal{K}(1 + |D|^2\mathcal{K}^2)} \\ &+ \frac{\mathcal{K}\left[|\delta - \xi\mathcal{K}D(\gamma - i\Omega)|^2 + 4\gamma^2|D|^2\left(\gamma_m^2 + \Omega^2\right)\right]}{(\gamma^2 + \Omega^2)(1 + |D|^2\mathcal{K}^2)}. \end{aligned} \tag{3.14}$$

It is reasonable to analyze three values of the pump level to simplify the solution. For the small enough pump we get

$$\mathcal{K}|D| \ll \left|\frac{\delta}{\gamma - i\Omega}\right| \tag{3.15a}$$

$$\text{or } \mathcal{K} \ll \mathcal{K}_{\text{crit1}} = \frac{\sqrt{\gamma_m^2 + \Omega^2}|\delta|}{|\Delta|}. \tag{3.15b}$$

In this case we omit terms $\xi\mathcal{K}D(\gamma - i\Omega)$ from the numerator and $|D|^2\mathcal{K}$ from the denominator of the last term in (3.14). The expression for the noise power spectral density transforms to

$$\begin{aligned} S(\Omega) &= 2\gamma_m(n_T + 1) + \frac{\gamma_m^2 + \Omega^2}{\mathcal{K}} \\ &+ \mathcal{K}\left(\frac{\delta^2}{\gamma^2 + \Omega^2} + \frac{4\gamma^2\Delta^2}{(\gamma^2 + \Omega^2)^2}\right). \end{aligned} \tag{3.16}$$

Here the last term describes the residual back action because of the frequency detunings.

We find the optimal pump parameter $\mathcal{K}_{\text{opt}}$ that minimizes (3.16) and present it in the form

$$\mathcal{K}_{\text{opt}} = \frac{\sqrt{\gamma_m^2 + \Omega^2}(\gamma^2 + \Omega^2)}{\sqrt{\delta^2(\gamma^2 + \Omega^2) + 4\gamma^2\Delta^2}}. \tag{3.17}$$

Comparison of $\mathcal{K}_{\text{opt}}$ with $\mathcal{K}_{\text{crit1}}$ shows that in order to satisfy (3.15b) the detunings have to obey the condition

$$\gamma^2\Delta^2 \ll \delta^2(\delta^2 + 4\Delta^2). \tag{3.18}$$

This is impossible if $|\Delta| \geqslant |\delta|$ since $|\delta| < \gamma$, per our initial assumption. Hence, in this case we can drop the back action term and the noise power spectral density (3.16) becomes

$$S(\Omega) = 2\gamma_m(n_T + 1) + \frac{\gamma_m^2 + \Omega^2}{\mathcal{K}}. \tag{3.19}$$

It reaches its minimum

$$S(\Omega) = 2\gamma_m(n_T + 1) + S_{\text{SQL},f}\frac{|\Delta|}{2|\delta|}, \tag{3.20}$$

when $\mathcal{K} \approx \mathcal{K}_{\text{crit1}}$.

In case $|\Delta| \ll |\delta|$ we find

$$S(\Omega) = 2\gamma_m(n_T + 1) + S_{\text{SQL},f}\frac{|\delta|}{\sqrt{\gamma^2 + \Omega^2}}. \tag{3.21}$$

For the case of a higher power pump

$$\mathcal{K}_{\text{crit2}} = \frac{\sqrt{\gamma^2 + \Omega^2}\sqrt{\gamma_m^2 + \Omega^2}}{\Delta} \gg \mathcal{K} \gg \mathcal{K}_{\text{crit1}} \tag{3.22}$$

we omit term δ from the numerator and $|D|^2\mathcal{K}$ from the denominator of the last term in (3.14). The noise power spectral density takes the form

$$S(\Omega) = 2\gamma_m(n_T+1) + \frac{\gamma_m^2+\Omega^2}{\mathcal{K}} + \mathcal{K}^3|D|^2. \qquad (3.23)$$

The optimal pump parameter $\mathcal{K}_{\rm opt}$, that minimizes (3.23), is

$$\mathcal{K}_{\rm opt} = \frac{\left(\gamma_m^2+\Omega^2\right)^{1/2}(\gamma^2+\Omega^2)^{1/4}}{3^{1/4}|\Delta|^{1/2}}. \qquad (3.24)$$

Comparison of $\mathcal{K}_{\rm opt}$ with $\mathcal{K}_{\rm crit1}$ and $\mathcal{K}_{\rm crit2}$ shows that in order to satisfy (3.22) the detunings have to follow the relation

$$1 \gg |\Delta|/\gamma \gg \delta^2/\gamma^2, \qquad (3.25)$$

which is feasible. The minimal noise power spectral density in this case equals to

$$S_{\rm min} = 2\gamma_m(n_T+1) + \left(3^{1/4}+\frac{1}{3^{1/4}}\right)\frac{\left(\gamma_m^2+\Omega^2\right)^{1/2}\Delta^{1/2}}{(\gamma^2+\Omega^2)^{1/4}} \qquad (3.26a)$$

$$= 2\gamma_m(n_T+1) + \frac{\sqrt{3}+1}{2\sqrt[4]{3}}\frac{\Delta^{1/2}}{(\gamma^2+\Omega^2)^{1/4}}S_{{\rm SQL},f}. \qquad (3.26b)$$

Finally, for the large pump power

$$\mathcal{K}|D| \gg 1, \quad \text{or } \mathcal{K} \gg \mathcal{K}_{\rm crit2}, \qquad (3.27)$$

we omit term δ from the numerator and 1 from the denominator of the last term in (3.14). Noise power spectral density takes the form

$$S(\Omega) = 2\gamma_m(n_T+1) + \mathcal{K} + \frac{4\gamma^2\left(\gamma_m^2+\Omega^2\right)}{\mathcal{K}(\gamma^2+\Omega^2)}. \qquad (3.28)$$

The optimal pump parameter $\mathcal{K}_{\rm opt}$ minimizing (3.28) becomes

$$\mathcal{K}_{\rm opt} = \sqrt{\frac{4\gamma^2\left(\gamma_m^2+\Omega^2\right)}{(\gamma^2+\Omega^2)}}. \qquad (3.29)$$

Comparison of $\mathcal{K}_{\rm opt}$ with $\mathcal{K}_{\rm crit2}$ shows that in order to satisfy (3.27) the detunings have to follow the relationship $1 \ll (2\Delta)/\gamma$, contradicting our assumption that $\Delta \ll \gamma$. Therefore, in this case the back action term proportional to the pump power dominates and the noise power spectral density (3.28) becomes

$$S(\Omega) \simeq 2\gamma_m(n_T+1) + \mathcal{K}. \qquad (3.30)$$

It reaches the minimum at $\mathcal{K} = \mathcal{K}_{\rm crit2}$ and its minimum is related to the SQL (2.33, 2.34) as

$$\begin{aligned} S(\Omega) &= 2\gamma_m(n_T+1) + \mathcal{K}_{\rm crit2} \\ &= 2\gamma_m(n_T+1) + S_{{\rm SQL},f}\frac{\sqrt{\gamma^2+\Omega^2}}{2\Delta}. \end{aligned} \qquad (3.31a)$$

Comparing the results (3.20), (3.21), (3.26), and (3.31) we find that the regime of the intermediate pump power provides the minimal noise spectral density for the case of $|\Delta| \gg |\delta|$, while for the opposite case, $|\Delta| \ll |\delta|$, the limit of smaller power is optimal.

IV. COHERENT COUPLING AND QUANTUM-MECHANICS-FREE SUBSYSTEMS

In this section we discuss in detail the fundamental features of the scheme proposed here that lead to the back action evasion. We show that the here proposed measurement strategy is analogous to the quantum-mechanics-free subsystem-based QND measurement technique. This is another important result of our paper.

A. Coherent coupling

It is possible to argue that our measurement technique realizes coherent coupling, proposed in [41], between the optical modes and the mechanical mode. Unlike the traditional dispersive coupling, in our case the mechanical displacement does not affect the frequencies of the optical modes. Instead, it rotates the basis vectors of amplitude distribution coefficients.

A ring resonator with a partially reflective mirror [41] is an example of the coherent coupling. The mirror lifts the degeneracy between the clockwise and anticlockwise modes in this resonator and creates the new symmetric and antisymmetric eigenmodes with the point of the node and antinode on the input mirror. Displacement x of this mirror shifts the position of this point by x, which can be considered as the rotation of the basis vectors representing the eigenmodes, without change of the eigenfrequencies.

Let us start from the Hamiltonian of the scheme, written in the matrix form

$$H = \hbar(\hat c_0\ \hat c_+\ \hat c_-)^\dagger \begin{pmatrix} \omega_0 & i\eta^*\hat d^\dagger & -i\eta\hat d \\ -i\eta\hat d & \omega_+ & 0 \\ i\eta^*\hat d^\dagger & 0 & \omega_- \end{pmatrix}\begin{pmatrix}\hat c_0\\ \hat c_+\\ \hat c_-\end{pmatrix}. \qquad (4.1)$$

Considering the mechanical mode operator $\hat d$ as a parameter d, we diagonalize the matrix and find the eigenfrequencies of the system:

$$(\omega_0-\lambda)(\omega_+-\lambda)(\omega_--\lambda) - 2|\eta d|^2(\omega-\lambda) = 0, \qquad (4.2a)$$

$$(\omega_0-\lambda)\left[(\omega_\lambda)^2 - \omega_m^2 - 2|\eta d|^2\right] = 0, \qquad (4.2b)$$

$$\lambda_1 = \omega_0, \qquad (4.2c)$$

$$\lambda_{2,3} = \omega \pm \sqrt{\omega_m^2 + 2|\eta d|^2} \approx \omega \pm \omega_m = \omega_\pm. \qquad (4.2d)$$

In the linear approximation the eigenfrequencies $\lambda_{1,2,3}$ do not depend on the mechanical degree of freedom d. Eigenmodes $\hat c_{1,2,3}$, corresponding to the eigenfrequencies $\lambda_{1,2,3}$, in linear approximation, can be expressed via initial (partial) modes as

$$\hat c_1 = \left(1,\ \frac{i\eta d}{\omega_m},\ \frac{i\eta^* d^*}{\omega_m}\right)\begin{pmatrix}\hat c_0\\ \hat c_+\\ \hat c_-\end{pmatrix}, \qquad \mathbf{v}_1 = \left(1,\ \frac{i\eta d}{\omega_m},\ \frac{i\eta^* d^*}{\omega_m}\right),$$

$$\hat c_2 = \left(\frac{i\eta^* d^*}{\omega_m},\ 1,\ 0\right)\begin{pmatrix}\hat c_0\\ \hat c_+\\ \hat c_-\end{pmatrix}, \qquad \mathbf{v}_2 = \left(\frac{i\eta^* d^*}{\omega_m},\ 1,\ 0\right),$$

$$\hat c_3 = \left(\frac{i\eta d}{\omega_m},\ 0,\ 1\right)\begin{pmatrix}\hat c_0\\ \hat c_+\\ \hat c_-\end{pmatrix}, \qquad \mathbf{v}_3 = \left(\frac{i\eta d}{\omega_m},\ 0,\ 1\right). \qquad (4.3)$$

This expression can be explained in terms of the coherent coupling concept. If $d = 0$ (the mechanical oscillator is in equilibrium), the eigenmodes transform into the initial optical modes $\hat{c}_1 \to \hat{c}$, $\hat{c}_2 \to \hat{c}_+$, and $\hat{c}_3 \to \hat{c}_-$, which allows us to use them in our analysis.

Parameters $\mathbf{v}_{1,2,3}$ are the vectors of amplitude distribution coefficients. In linear approximation they are orthogonal and have constant norm equal to 1: $(\mathbf{v}_i, \mathbf{v}_j) = \delta_{ij} + O(d^2)$. Thus the coupling between optical and mechanical modes does not change the lengths of the basis vectors, rotating them instead.

Let us compare our scheme with a similar scheme proposed earlier [34]. It is based on the Michelson-Sagnac interferometer (MSI) with a partially transparent mirror. It also has two nondegenerate optical modes and the movement of the mirror provides the coupling between them. In that scheme we analyze its Hamiltonian (again we consider the mechanical mode operator $\hat{d}$ as a C number):

$$H = \hbar(\hat{c}_+\ \hat{c}_-)^\dagger \begin{pmatrix} \omega_+ & -i\eta d \\ i\eta^* d^* & \omega_- \end{pmatrix} \begin{pmatrix} \hat{c}_+ \\ \hat{c}_- \end{pmatrix}. \tag{4.4}$$

The eigenfrequencies of this system are

$$\lambda_{1,2} = \omega_+ + \omega_- \pm \sqrt{(\omega_+ - \omega_-)^2 + 4|\eta d|^2} \approx \omega_\pm. \tag{4.5}$$

The corresponding eigenmodes can be expressed via initial modes as

$$\hat{c}_1 = \left(1,\ \frac{i\eta d}{\omega_m}\right)\begin{pmatrix} \hat{c}_+ \\ \hat{c}_- \end{pmatrix}, \tag{4.6a}$$

$$\hat{c}_2 = \left(\frac{i\eta^* d^*}{\omega_m},\ 1\right)\begin{pmatrix} \hat{c}_+ \\ \hat{c}_- \end{pmatrix}. \tag{4.6b}$$

Therefore, this system also represents the coherent coupling. The difference between the schemes is in the interaction structure. It the scheme proposed here the optical sidebands $c_\pm$ do not interact with each other directly; instead, the interaction goes on via the central mode c. Moreover, the eigenmode of the sideband c_2 (or c_3) does not depend on the partial mode of the respective opposite sideband c_- (or c_+).

In the scheme described in [34] there is no intermediate mode, so the two modes have to interact with each other. It leads to an instability due to the ponderomotive nonlinearity. Our scheme is free of instability, thanks to the presence of the central mode c_0.

B. QMFS and back action evasion

To explain how back action evasion is realized in our scheme we present our system in terms of the QMFS, introduced in [40]. A set of variables $\{X_1, ...X_n\}$ forms a QMFS if

$$\forall i,\ j,\ \forall t, t'\ [X_i(t), X_j(t')] = 0. \tag{4.7}$$

In this case the measurement of a variable X_i at time t does not perturb any of the variables X_j $(i \neq j)$ from the set and they can be precisely measured at time t'.

Since the quantities that we observe in the experiment are quadrature amplitudes, to identify independent QMFSs for our system we have to present the Hamiltonian in terms of the observables. We provide a simplified description of the procedure in this section, while the strict and detailed derivation can be found in Appendix B.

We start from the equations of motion (2.23) for the quadrature amplitudes and remove the decay and pump, which corresponds to the analysis of a closed system:

$$\dot{c}_{+a} = -\eta C_0 d_a, \tag{4.8a}$$

$$\dot{c}_{+\phi} = -\eta C_0 d_\phi, \tag{4.8b}$$

$$\dot{c}_{-a} = \eta C_0 d_a, \tag{4.8c}$$

$$\dot{c}_{-\phi} = -\eta C_0 d_\phi, \tag{4.8d}$$

$$\dot{d}_a = \eta C_0 (c_{+a} + c_{-a}), \tag{4.8e}$$

$$\dot{d}_\phi = \eta C_0 (c_{+\phi} - c_{-\phi}). \tag{4.8f}$$

These equations of motion are generated by the Hamiltonian

$$V = \hbar\eta C_0 (c_{+a} + c_{-a}) d_a + \hbar\eta C_0 (c_{+\phi} - c_{-\phi}) d_\phi \tag{4.9}$$

[it coincides with (B7) derived in Appendix B]. We introduce

$$d_a = Q, \quad d_\phi = P, \tag{4.10}$$

$$\frac{c_{+a} + c_{-a}}{\sqrt{2}} = \Phi_1, \quad \frac{c_{+\phi} + c_{-\phi}}{\sqrt{2}} = \Pi_1, \tag{4.11}$$

$$\frac{c_{+a} - c_{-a}}{\sqrt{2}} = \Phi_2, \quad \frac{c_{+\phi} - c_{-\phi}}{\sqrt{2}} = \Pi_2. \tag{4.12}$$

Operators Q and P, as well as $\Phi_{1,2}$ and $\Pi_{1,2}$, are quantum conjugated, that is,

$$[Q, P] = [\Phi_1, \Pi_1] = [\Phi_2, \Pi_2] = i\delta_{jk}. \tag{4.13}$$

The other variables of the system commute with each other. We can rewrite the Hamiltonian as

$$V = \sqrt{2}\hbar|\eta C|\Phi_1 Q + \sqrt{2}\hbar|\eta C|\Pi_2 P. \tag{4.14}$$

The equations of motions are

$$\dot{\Pi}_1 = \sqrt{2}|\eta C|Q, \quad \dot{Q} = \sqrt{2}|\eta C|\Pi_2, \quad \dot{\Pi}_2 = 0, \tag{4.15}$$

$$\dot{\Phi}_2 = \sqrt{2}|\eta C|P, \quad \dot{P} = -\sqrt{2}|\eta C|\Phi_1, \quad \dot{\Phi}_1 = 0. \tag{4.16}$$

Their solution in the time domain is

$$\begin{aligned} \Pi_1 &= \Pi_{10} + \sqrt{2}|\eta C|Q_0 t + |\eta C|^2 \Pi_{20} t^2, \\ Q &= Q_0 + \sqrt{2}|\eta C|\Pi_{20} t,\ \Pi_2 = \Pi_{20}, \end{aligned} \tag{4.17}$$

$$\begin{aligned} \Phi_2 &= \Phi_{20} + \sqrt{2}|\eta C|P_0 t - |\eta C|^2 \Phi_{10} t^2, \\ P &= P_0 - \sqrt{2}|\eta C|\Phi_{10} t,\ \Phi_1 = \Phi_{10}. \end{aligned} \tag{4.18}$$

Here $X_0 = X(0)$ for each variable $X(t)$.

As we can see, every variable from this system is a QND variable. It is due to the fact that none of them depend dynamically on their conjugate. Moreover, all of the variables from the upper (4.17) [or lower (4.18)] set commute with each other. That is why they form the QMFS. Therefore, we have two independent (in the dynamic sense) QMFSs: $\{\Pi_1,\ Q,\ \Pi_2\}$ and $\{\Phi_2,\ P,\ \Phi_1\}$.

Let us consider the subsystem $\{\Pi_1,\ Q,\ \Pi_2\}$ (4.17). The meaning of each term in the equation for Π_1 is as follows. Π_{10} corresponds to shot noise, $\sqrt{2}|\eta C|Q_0 t$ corresponds to the signal, and $|\eta C|^2 \Pi_{20} t^2$ is the back action. We recall that $\Pi_1 = \frac{c_{+\phi} + c_{-\phi}}{\sqrt{2}}$ and $\Pi_2 = \frac{c_{+\phi} - c_{-\phi}}{\sqrt{2}}$. It happens because this system has two outputs and two phase quadrature amplitudes of the output fields, corresponding to c_p and c_m. We can independently take their sum (Π_1) and difference (Π_2) and perform a quantum demolition measurement of $Q = d_a$, which would allow us to get the information about the signal force acting on that quadrature.

We have removed the decay and pump terms and considered the closed system in the analysis presented above, to explain how the QMFSs appear in this scheme. The analysis of the realistic scheme presented in Sec. II B is in full agreement with this consideration.

It is interesting to compare our scheme with the measurement scheme based on "negative mass" by Tsang and Caves (TC) [40]. The Hamiltonian of their general model is

$$V_{\rm TC} = \frac{m\omega^2 q^2}{2} + \frac{p^2}{2m} - \frac{m\omega^2 q'^2}{2} - \frac{p'^2}{2m}. \tag{4.19}$$

The observable variables that correspond to real physical systems are $\{q,\ p\}$ (for example, coordinate and momentum of a mechanical oscillator) and $\{q',\ p'\}$ (for example, quadratures of the auxiliary optical resonator). The force acts on q. None of these variables is QND. The QND variables are

$$q + q' = Q_{\rm TC}, \qquad \frac{p + p'}{2} = P_{\rm TC}, \tag{4.20}$$

$$\frac{q - q'}{2} = \Phi_{\rm TC}, \qquad p - p' = \Pi_{\rm TC}. \tag{4.21}$$

Measuring $Q_{\rm TC}$ would allow one to get the information about the signal force and avoid the back action.

The scheme of the broadband variation measurement proposed here has several distinguishing features.

(a) All of its variables are already of QND nature.

(b) These QND variables Q, P, $\Phi_{1,2}$, and $\Pi_{1,2}$ correspond to parameters of real physical systems (Q and P are the quadrature amplitudes of the mechanical oscillator, and $\Phi_{1,2}$ and $\Pi_{1,2}$ are quadrature amplitudes of the optical modes).

(c) There are three degrees of freedom in our scheme (two optical and one mechanical), whereas in the scheme of [40] only two degrees of freedom are considered. The presence of the three degrees of freedom enables measurements of the optical quadratures in the two channels and results in the cancellation of the back action in a broad band.

(d) The variables $\Phi_{1,2}$ and $\Pi_{1,2}$ correspond to the probes, while in the scheme of [40] measurement of $Q_{\rm TC}$ has to be made with an additional probe.

V. DISCUSSION

In this paper we have introduced a broadband back action evading measurement of a classical mechanical force. In the measurement scheme described by Fig. 1 the signal information contained in the mechanical *quadratures* transfers to the optical quadratures. The measurement of the difference of the optical amplitude quadratures is equivalent to the registration of the mechanical amplitude quadrature, whereas the measurement of the sum of the optical phase quadratures corresponds to the registration of the mechanical phase quadrature, as shown by Eq. (2.23). This is a peculiar property of the parametric interaction. One of the main features of the here proposed measurement strategy is the usage of the single probe field with detection in the two independent quantum outputs. It gives us a flexibility to measure back action separately and then subtract it completely from the measurement result. The subtraction of back action can be made in a broad frequency band.

In contrast, in conventional variational measurements [25–27] there is only one quantum output and the back action cannot be measured separately from the signal. Measurement of the linear combination of the amplitude and phase quadratures in that case allows partial subtraction of the back action. Only one quadrature of the output wave has to be measured to surpass the SQL.

The scheme proposed here allows a measurement of a combination of either the sum and difference of amplitude quadratures (2.30) or the sum and difference of phase quadratures (2.36). Generalization (2.37) is also possible. These measurements lead to back action evasion in a broad frequency band. We expect that this technique will find a realization in other configurations.

Our paper represents the further development of the broadband dichromatic variational measurement [34]. The main advantages of the current paper include the following.

(i) Our scheme uses one optical pump, in contrast with the two pumps considered in [34].

(ii) The configuration proposed in [34] requires compensation of the resonant classical mechanical force impinged by the dichromatic pump on the mechanical oscillator. Our scheme is free of it.

(iii) The configuration proposed here is free from parasitic back action, which takes place in the scheme of [34].

It worth noting that a similar idea was recently considered in the electro-optical configuration [42]. However, in that case the classical force depended on the attenuation of a radio-frequency system, while in our case there is no such dependence. Additionally, here we have considered a nonideal case involving various frequency detunings and found the validity range of the technique.

Physical realizations

We have considered the three-mode scheme, as shown in Fig. 1. Let us introduce two physical realizations described by the Hamiltonian (2.2) and Langevin equations (2.4)—two-mode and three-mode schemes.

1. Three-mode scheme

One of the possible realizations of the three-mode scheme is shown on Fig. 4. The short optical resonator with optical length L_0 is located in the middle of the long optical resonator with optical length $2L + L_0$. The short optical resonator is considered as the test mass of the mechanical oscillator and moves as a whole. One can use a thin membrane with two reflective coatings with transmissivity t and reflectivity r to reduce the mass m and increase the eigenfrequency ω_m of the oscillator.

To work with this scheme the following conditions have to be met.

(1) The optical lengths L_0 and L have to be chosen so that the middle mode ω_0 is in resonance with all particle

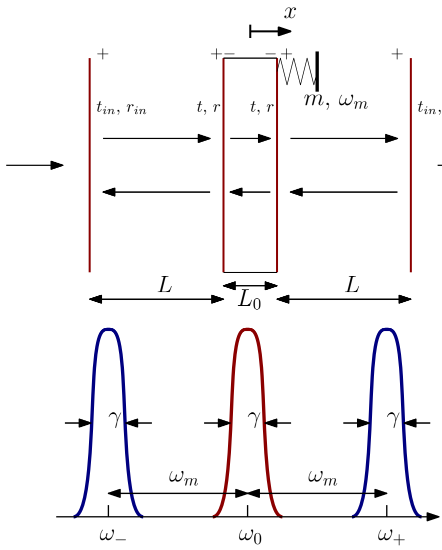

FIG. 4. Three-mode scheme enabling the broadband QND measurement.

resonators:

$$e^{2i\omega_0 L_0/c} = e^{2i\omega_0 L/c} = 1. \tag{5.1}$$

(2) The thin membrane has to be located in the middle of the long resonator. Its optical length L_0 has to be smaller than the optical length $2L + L_0$ of the long resonator so that

$$L_0 \ll L. \tag{5.2}$$

(3) The transmissivity $t_{\rm in}$ of the end mirrors has to be smaller than the transmissivity t of the membrane surface coating to save the mode structure:

$$t_{\rm in} \ll t. \tag{5.3}$$

Under these conditions the system has the desired three-mode structure with the interaction Hamiltonian:

$$\hat{H}_{\rm int} = \hbar\eta[c_0(dc_+^\dagger + d^\dagger c_-^\dagger) + c_0^\dagger(d^\dagger c_+ + dc_-)], \tag{5.4a}$$

$$\eta = \frac{\omega_0 x_0\sqrt{L_0}}{\sqrt{L^3}}, \tag{5.4b}$$

which has a form similar to (2.2b) at substitution $c_0 \to -ic_0$, $c_0^\dagger \to ic_0^\dagger$ ($\pi/2$ phase shift). The details of derivation can be found in Appendix C.

It is worth noting that other realizations of the triply resonant schemes are feasible.

2. Two-mode scheme

Interestingly, we also can use the two-mode scheme with frequencies $\omega_0 \pm \omega_m$ and use the pump with frequency ω_0 located in between the modes.

As an example we consider a system based on the MSI shown in Fig. 5. It has two degenerate modes. If the position of a perfectly reflecting mirror M is fixed, one MSI mode, characterized with frequency ω_+, is given by a light wave which travels between M_1 and the beam splitter. The light is split on the beam splitter and after reflection from mirror M returns exactly to M_1. It does not propagate to M_2. The other mode, characterized with frequency ω_-, is represented by a wave which travels from M_2 to the beam splitter and after reflection from M returns to M_2 and does not propagate to M_1. The frequencies of the modes, $\omega_\pm$, are controlled by variation of path distances ℓ_1 and ℓ_2.

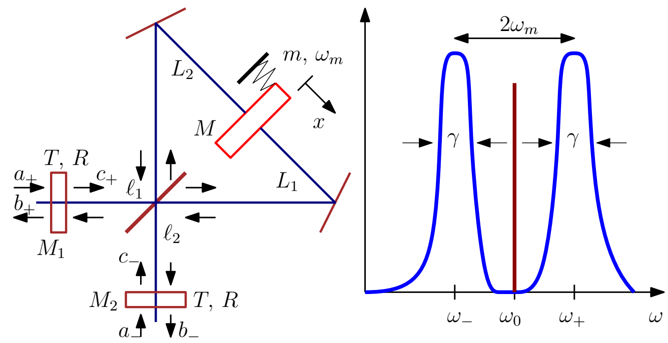

FIG. 5. Two-mode scheme.

Variation of the position x of mirror M provides coupling between the modes. Mirror M is a test mass of the mechanical oscillator with mass m and eigenfrequency ω_m. The back action can be suppressed in this scheme as well. However, the pump on frequency ω_0 is not resonant and more optical power will be needed to beat the SQL as compared with the resonant pump. In particular, the power of the pump laser must be larger by $\simeq 2/\gamma\tau$ times (τ is round trip time in cavity ω_0). In addition the pump should be excited through both mirrors M_1 and M_2.

The system is described with a Hamiltonian similar to (2.2b):

$$H_{\rm int} = \frac{\hbar\tilde{\eta}|C|}{i}(\hat{d}[\hat{c}_- + \hat{c}_+^\dagger] - \hat{d}^\dagger[\hat{c}_-^\dagger + \hat{c}_+]), \tag{5.5}$$

$$\tilde{\eta} = \frac{\tilde{\omega}x_0}{\tilde{\ell}}, \tag{5.6}$$

where $|C|$ is the amplitude of the pump (see details in Appendix D). So all consideration above in the paper is valid for the two-mode scheme.

VI. CONCLUSION

We have shown that the simultaneous and independent measurements of optimal quadrature amplitudes of two optical harmonics generated due to ponderomotive interaction of light and a mechanical force mediated by an optomechanical interaction enable a back action evading measurement. The back action can be removed from the signal by postprocessing of the measurement data. The measurement becomes feasible since the optomechanical system is an example of the quantum configuration containing quantum-mechanics-free subsystems lending themselves to continuous quantum nondemolition measurements [40].

In this paper we consider the interaction of *two* optical modes (plus a third pump mode) with *one* mechanical degree of freedom. Another possibility is interaction of *one* optical mode with *two* mechanical ones [43]. It would be interesting to compare advantages and drawbacks of these approaches.

We hope that the here proposed broadband coherent multidimensional variational measurement can be used in precision optomechanical measurements including laser gravitational wave detectors.

ACKNOWLEDGMENTS

The research of S.P.V. and A.I.N. has been supported by the Russian Foundation for Basic Research (Grant No. 19-29-11003), by Theoretical Physics and Mathematics Advancement Foundation "BASIS" (Grant No. 22-1-1-47-1), by the Interdisciplinary Scientific and Educational School of Moscow University "Fundamental and Applied Space Research," and by the TAPIR GIFT MSU Support of the California Institute of Technology. A.I.N. is the recipient of a Theoretical Physics and Mathematics Advancement Foundation "BASIS" scholarship (Grant No. 21-2-10-47-1). Research performed by A.B.M. was carried out at the Jet Propulsion Laboratory, California Institute of Technology, under a contract with the National Aeronautics and Space Administration (Grant No. 80NM0018D0004). This paper has LIGO No. P2200131.

APPENDIX A: DERIVATION OF THE INTRACAVITY FIELDS

In this Appendix we provide details of the standard calculation for intracavity fields (for example, see [44]).

We begin with Hamiltonian (2.2):

$$H_T = \sum_{k=0}^{\infty} \hbar\omega_k b_k^\dagger b_k, \tag{A1}$$

$$H_\gamma = i\hbar\sqrt{\frac{\gamma\Delta\omega}{\pi}}\sum_{k=0}^{\infty}[(c_+^\dagger + c_-^\dagger)b_k - (c_+ + c_-)b_k^\dagger],$$

$$H_{T,m} = \sum_{k=0}^{\infty} \hbar\omega_k q_k^\dagger q_k, \tag{A2}$$

$$H_{\gamma_m} = i\hbar\sqrt{\frac{\gamma\Delta\omega}{\pi}}\sum_{k=0}^{\infty}[d^\dagger q_k - d q_k^\dagger]. \tag{A3}$$

Here H_T is the Hamiltonian of the environment presented as a bath of oscillators described with frequencies $\omega_k = \omega_{k-1} + \Delta\omega$ and annihilation and creation operators b_k and $b_k^\dagger$. H_γ is the Hamiltonian of coupling between the environment and the optical resonator, and γ is the coupling constant. Similarly $H_{T,m}$ is the Hamiltonian of the environment presented by a thermal bath of mechanical oscillators with frequencies $\omega_k = \omega_{k-1} + \Delta\omega$ and amplitudes described with annihilation and creation operators q_k and $q_k^\dagger$. H_{γ_m} is the Hamiltonian of coupling between the environment and the mechanical oscillator, and $2\gamma_m$ is the decay rate of the oscillator.

We write Heisenberg equations for operators c_+ and b_k:

$$i\hbar\dot{c}_+ = [c_+, H] = \hbar\omega_+ c_+ - i\hbar\eta c_- d + i\hbar\sqrt{\frac{\gamma\Delta\omega}{\pi}}\sum_{k=0}^{\infty} b_k, \tag{A4a}$$

$$i\hbar\dot{b}_k = [b_k, H] = \hbar\omega_k b_k - i\hbar\sqrt{\frac{\gamma\Delta\omega}{\pi}}(c_+ + c_-). \tag{A4b}$$

We introduce slow amplitudes $c_\pm \to c_\pm e^{-i\omega_\pm t}$, $d \to d e^{-i(\omega_+ - \omega_-)t}$, and $b_k \to b_k e^{-i\omega_k t}$ and substitute them into (A4):

$$\dot{c}_+ = -\eta c_- d + \sqrt{\frac{\gamma\Delta\omega}{\pi}}\sum_{k=0}^{\infty} b_k e^{-i(\omega_k - \omega_+)t}, \tag{A5a}$$

$$\dot{b}_k = -\sqrt{\frac{\gamma\Delta\omega}{\pi}}(c_+ e^{-i(\omega_+ - \omega_k)t} + c_- e^{-i(\omega_- - \omega_k)t}). \tag{A5b}$$

Using initial condition $b_k(t=0) = b_k(0)$ to integrate (A5b) we derive

$$b_k(t) = b_k(0) - \int_0^t \sqrt{\frac{\gamma\Delta\omega}{\pi}} c_+(s) e^{-i(\omega_+ - \omega_k)s} ds \tag{A6}$$

$$- \int_0^t \sqrt{\frac{\gamma\Delta\omega}{\pi}} c_-(s) e^{-i(\omega_- - \omega_k)s} ds. \tag{A7}$$

Using the condition $b_k(t=\infty) = b_k(\infty)$ to integrate (A5b) we derive

$$b_k(t) = b_k(\infty) + \int_t^\infty \sqrt{\frac{\gamma\Delta\omega}{\pi}} c_+(s) e^{-i(\omega_+ - \omega_k)s} ds \tag{A8}$$

$$+ \int_t^\infty \sqrt{\frac{\gamma\Delta\omega}{\pi}} c_-(s) e^{-i(\omega_- - \omega_k)s} ds. \tag{A9}$$

To get the input-output relation we substitute initial condition (A7) into (A5a),

$$\dot{c}_+ = -\eta c_- d + \sum_{k=0}^{\infty}\sqrt{\frac{\gamma\Delta\omega}{\pi}} b_k(0) e^{-i(\omega_k - \omega_+)t} \tag{A10a}$$

$$- \sum_{k=0}^{\infty}\int_0^t \frac{\gamma\Delta\omega}{\pi} c_+(s) e^{-i(\omega_k - \omega_+)(t-s)} ds$$

$$- \left(\sum_{k=0}^{\infty}\int_0^t \frac{\gamma\Delta\omega}{\pi} c_-(s) e^{-i(\omega_k - \omega_-)(t-s)} ds\right) e^{i(\omega_+ - \omega_-)t}, \tag{A10b}$$

omit the last term proportional to $e^{i(\omega_+ - \omega_-)t}$ as the fast oscillating term, and define the input field:

$$a_+(t) = \sum_{k=0}^{\infty}\sqrt{\frac{\Delta\omega}{2\pi}} b_k(0) e^{-i(\omega_k - \omega_+)t}. \tag{A11}$$

To calculate the remaining sum in (A10) we assume the validity of limit $\Delta\omega \to 0$ and replace the sum by the integration

$$\Delta\omega \sum_{k=0}^{\infty} \to \int_0^\infty d\omega_k \tag{A12a}$$

$$\sum_{k=0}^{\infty}\int_0^t \frac{\gamma\Delta\omega}{\pi} c_+(s) e^{-i(\omega_k - \omega_+)(t-s)} ds \tag{A12b}$$

$$\to \int_0^\infty \int_0^t 2\gamma c_+(s) e^{-i(\omega_k - \omega_+)(t-s)} ds \frac{d\omega_k}{2\pi}$$

$$= \int_{-\omega_+}^\infty \int_0^t 2\gamma c_+(s) e^{-i\omega(t-s)} ds \frac{d\omega}{2\pi}$$

$$\approx \int_{-\infty}^\infty \int_0^t 2\gamma c_+(s) e^{-i\omega(t-s)} ds \frac{d\omega}{2\pi}$$

$$= \int_0^t 2\gamma c_+(s)\delta(t-s)ds = \frac{2\gamma c_+(t)}{2} = \gamma c_+(t). \tag{A12c}$$

Substituting (A11) and (A12) into (A10) we obtain

$$\dot{c}_+ = -\eta c_- d + \sqrt{2\gamma} a_+ - \gamma c_+, \tag{A13}$$

$$\dot{c}_+ + \gamma c_+ + \eta c_- d = \sqrt{2\gamma} a_+. \tag{A14}$$

By analogy, we derive the equation for input field a_- and present it in a similar form:

$$a_-(t) = \sum_{k=0}^{\infty} \sqrt{\frac{\Delta\omega}{2\pi}} b_k(0) e^{-i(\omega_k - \omega_-)t}. \tag{A15}$$

It leads to the equation for the intracavity field c_-:

$$\dot{c}_- + \gamma c_- - \eta c_+ d^\dagger = \sqrt{2\gamma} a_-. \tag{A16}$$

A similar equation can be derived for the amplitude $q(t)$ of the mechanical oscillator,

$$q(t) = \sum_{k=0}^{\infty} \sqrt{\frac{\Delta\omega}{2\pi}} b_{m,k}(0) e^{-i(\omega_k - \omega_+)t}, \tag{A17}$$

resulting in the Langevin equation for mechanical oscillator quadrature d:

$$\dot{d} + \gamma_m d - \eta^* c_+ c_-^\dagger = \sqrt{2\gamma_m} q. \tag{A18}$$

To derive the output relation we substitute (A9) into (A5a) and define the output fields:

$$b_+(t) = -\sum_{k=0}^{\infty} \sqrt{\frac{\Delta\omega}{2\pi}} b_k(\infty) e^{-i(\omega_k - \omega_+)t}, \tag{A19}$$

$$b_-(t) = -\sum_{k=0}^{\infty} \sqrt{\frac{\Delta\omega}{2\pi}} b_k(\infty) e^{-i(\omega_k - \omega_+)t}. \tag{A20}$$

It leads to

$$\dot{c}_+ - \gamma c_+ + \eta c_- d = \sqrt{2\gamma} b_+, \tag{A21}$$

$$\dot{c}_- - \gamma c_- + \eta^* c_+ d^\dagger = \sqrt{2\gamma} b_-. \tag{A22}$$

Utilizing pairs of equations (A14) and (A21) as well as (A16) and (A22) we obtain the final expression for the input-output relations:

$$b_+ = -a_+ + \sqrt{2\gamma} c_+, \tag{A23}$$

$$b_- = -a_- + \sqrt{2\gamma} c_-. \tag{A24}$$

Let us derive the commutation relations for the Fourier amplitudes of the operators. We introduce the Fourier transform of field $a_+(t)$ using (A11):

$$a_+(\Omega) = \int_{-\infty}^{\infty} \sum_{k=0}^{\infty} \sqrt{\frac{\Delta\omega}{2\pi}} b_k(0) e^{-i(\omega_k - \omega_+ - \Omega)t} dt \tag{A25a}$$

$$= \sum_{k=0}^{\infty} \sqrt{2\pi\,\Delta\omega} b_k(0) \delta(\Omega - \omega_k + \omega_+). \tag{A25b}$$

This allows us to find the commutators (2.16),

$$\begin{aligned}
[a_+(\Omega), a_+^\dagger(\Omega')] &= \sum_{k=0}^{\infty} 2\pi\,\Delta\omega [b_k(0), b_k^\dagger(0)] \\
&\quad \times\ \delta(\Omega - \omega_k + \omega_+)\delta(\Omega' - \omega_k + \omega_+) \\
&\quad \to \int_{-\infty}^{\infty} 2\pi [b(0), b^\dagger(0)] \\
&\quad \times\ \delta(\Omega - \omega)\delta(\Omega' - \omega) d\omega \\
&= 2\pi\delta(\Omega - \Omega'),
\end{aligned} \tag{A26}$$

and the correlators (2.17):

$$\begin{aligned}
&\langle a_+(\Omega), a_+^\dagger(\Omega')\rangle \\
&= \sum_{k=0}^{\infty} 2\pi\,\Delta\omega \langle b_k(0), b_k^\dagger(0)\rangle \\
&\times \delta(\Omega - \omega_k + \omega_+)\delta(\Omega' - \omega_k + \omega_+) \\
&\to \int_{-\infty}^{\infty} 2\pi \langle b(0), b^\dagger(0)\rangle \delta(\Omega - \omega)\delta(\Omega' - \omega) d\omega \\
&= 2\pi\delta(\Omega - \Omega').
\end{aligned} \tag{A27}$$

Similar expressions can be derived for commutators and correlators of the optical a_- and mechanical q quantum amplitudes.

APPENDIX B: HAMILTONIAN PRESENTED USING QUADRATURE AMPLITUDES

We start from the Hamiltonian describing the interaction of the modes of a lossless nonlinear cavity. We assume that all of the field operators (denoted by hats) depend on time:

$$H_0 = \hbar\omega \hat{c}^\dagger \hat{c} + \hbar\omega_- \hat{c}_-^\dagger \hat{c}_- + \hbar\omega_+ \hat{c}_+^\dagger \hat{c}_+ + \hbar\omega_m \hat{d}^\dagger \hat{d}, \tag{B1a}$$

$$V = \hbar\eta(\hat{c}_-^\dagger \hat{d}^\dagger + \hat{c}_+^\dagger \hat{d})\hat{c} + \hbar\eta^*(\hat{c}_- \hat{d} + \hat{c}_+ \hat{d}^\dagger)\hat{c}^\dagger. \tag{B1b}$$

From the analysis made earlier it is known that small fluctuations of the $\hat{c}$ mode do not influence the system. We change it to mean field $\hat{c} \to C$ and omit the term in H_0 connected to it. For all of the other modes the resonator is closed.

We express the creation and annihilation operators via their corresponding quadratures:

$$\hat{c}_\pm = \frac{\hat{c}_{\pm a} + i\hat{c}_{\pm\phi}}{\sqrt{2}}, \quad \hat{d} = \frac{\hat{d}_a + i\hat{d}_\phi}{\sqrt{2}}, \tag{B2a}$$

$$\hat{c}_\pm^\dagger = \frac{\hat{c}_{\pm a} - i\hat{c}_{\pm\phi}}{\sqrt{2}}, \quad \hat{d}^\dagger = \frac{\hat{d}_a - i\hat{d}_\phi}{\sqrt{2}}. \tag{B2b}$$

The Hamiltonian transforms to

$$H_0 = \frac{\hbar\omega_-}{2}(\hat{c}_{-a}^2 + \hat{c}_{-\phi}^2) + \frac{\hbar\omega_+}{2}(\hat{c}_{+a}^2 + \hat{c}_{+\phi}^2) + \frac{\hbar\omega_m}{2}(\hat{d}_a^2 + \hat{d}_\phi^2), \tag{B3a}$$

$$\begin{aligned}
V = &\frac{\hbar(\eta C + \eta^* C^*)}{2}[(\hat{c}_{-a} + \hat{c}_{+a})\hat{d}_a + (\hat{c}_{+\phi} - \hat{c}_{-\phi})\hat{d}_\phi] \\
&+ \frac{i\hbar(\eta^* C^* - \eta C)}{2}[(\hat{c}_{-\phi} + \hat{c}_{+\phi})\hat{d}_a + (\hat{c}_{-a} - \hat{c}_{+a})\hat{d}_\phi].
\end{aligned} \tag{B3b}$$

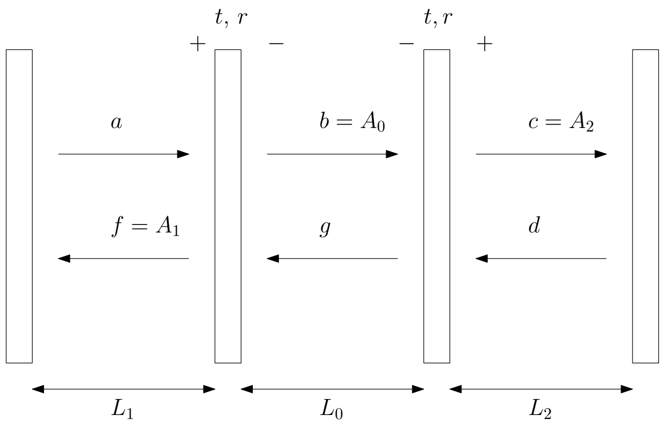

FIG. 6. Schematic of a cavity enabling a triplet of equidistant optical modes separated closely enough to interact with a resonant mechanical oscillator.

We assume that the coupling constant is real, $\eta = \eta^*$, and that the mean amplitude of the intracavity field is real, $C_0 = C_0^*$. Then $\eta C = \eta C_0 e^{-i\omega t}$, and the Hamiltonian transforms to

$$\begin{aligned} H_0 &= \frac{\hbar\omega_-}{2}\left(\hat c_{-a}^2 + \hat c_{-\phi}^2\right) + \frac{\hbar\omega_+}{2}\left(\hat c_{+a}^2 + \hat c_{+\phi}^2\right)\\ &\quad + \frac{\hbar\omega_m}{2}\left(\hat d_a^2 + \hat d_\phi^2\right),\\ V &= \hbar\eta C_0((\hat c_{+a} + \hat c_{-a})\cos\omega t - (\hat c_{+\phi} + \hat c_{-\phi})\sin\omega t)\hat d_a\\ &\quad + \hbar\eta C_0((\hat c_{+\phi} - \hat c_{-\phi})\cos\omega t + (\hat c_{+a} - \hat c_{-a})\sin\omega t)\hat d_\phi. \end{aligned} \tag{B4}$$

The Hamiltonian H_0 corresponds to the free evolution of the quadratures. It is instructive to introduce slow amplitudes

$$\hat c_{\pm a} = c_{\pm a}\cos\omega_\pm t + c_{\pm\phi}\sin\omega_\pm t, \tag{B5a}$$

$$\hat c_{\pm\phi} = c_{\pm\phi}\cos\omega_\pm t - c_{\pm a}\sin\omega_\pm t, \tag{B5b}$$

$$\hat d_a = d_a\cos\omega_m t + d_\phi\sin\omega_m t, \tag{B5c}$$

$$\hat d_\phi = d_\phi\cos\omega_m t - d_a\sin\omega_m t. \tag{B5d}$$

Using simple arithmetic we arrive at

$$\begin{aligned} \hat c_{\pm a}\cos\omega t - \hat c_{\pm\phi}\sin\omega t &= c_{\pm a}\cos\omega_m t \pm c_{\pm\phi}\sin\omega_m t,\\ \hat c_{\pm\phi}\cos\omega t + \hat c_{\pm a}\sin\omega t &= c_{\pm\phi}\cos\omega_m t \mp c_{\pm a}\sin\omega_m t. \end{aligned} \tag{B6}$$

Substituting these expressions into the interaction Hamiltonian V we get

$$V = \hbar\eta C_0(c_{+a} + c_{-a})d_a + \hbar\eta C_0(c_{+\phi} - c_{-\phi})d_\phi. \tag{B7}$$

APPENDIX C: DERIVATION OF THE INTERACTION HAMILTONIAN FOR THE THREE-MODE SCHEME

In this Appendix we provide the derivation of the interaction Hamiltonian for the three-mode scheme based on the four-mirror cavity structure shown in Fig. 6. End mirrors are fully reflective, and two mirrors in the middle are partially transparent with small transmissivity ($t \ll 1$). We assume that these two mirrors are the reflective coatings of a thin membrane.

We show that the three modes of this resonator are equidistant ($\delta k = k_+ - k_0 = k_0 - k_-$), the eigenfrequencies do not depend on the displacement of the membrane x, but the eigenmodes depend on and present the main stages of the derivation of the interaction Hamiltonian for this system.

1. The eigenfrequencies

The amplitudes of the fields in the different parts of the resonator are defined by the set of equations

$$\begin{aligned} &a = fe^{2ikL_1}, \quad b = ta - rg,\\ &c = tbe^{ikL_0} + rd, \quad d = ce^{2ikL_2},\\ &g = tde^{ikL_0} - rbe^{2ikL_0}, \quad f = tg + ra. \end{aligned} \tag{C1}$$

Determinant of the matrix of this set generates the characteristic equation

$$\begin{aligned} 1 - &e^{2ik(L_1+L_0+L_2)} - r(e^{2ikL_1} + e^{2ikL_2})(1 - e^{2ikL_0})\\ &+ r^2(e^{2ik(L_1+L_2)} - e^{2ikL_0}) = 0. \end{aligned} \tag{C2}$$

In the case of identical side resonators ($L_1 = L_2 = L$) Eq. (C2) turns into

$$e^{2ikL_0} = \left(\frac{1 - re^{2ikL}}{e^{2ikL} - r}\right)^2. \tag{C3}$$

Although in the general case this equation cannot be solved analytically, in the case of a thin membrane ($L_0 \ll L$) and cavity tuned to the resonance ($e^{2ik_0L_0} = e^{2ik_0L} = 1$) we can assume that the sideband frequencies are not too far from the middle mode frequency ($\delta kL \ll 1$) and simplify the characteristic equation (C3) as

$$1 + 2i\,\delta k\,L_0 \approx \left(\frac{\frac{t^2}{2} - 2i\,\delta k\,L}{\frac{t^2}{2} + 2i\,\delta k\,L}\right)^2. \tag{C4}$$

To simplify this equation further we assume that $\delta kL/t^2 \gg 1$. Then the right part of Eq. (C4) can be expanded, and we finally get

$$1 + 2i\,\delta k\,L_0 \simeq 1 - 4\left(\frac{t^2}{4i\,\delta k\,L}\right) \Rightarrow \delta k^2 \simeq \frac{t^2}{2LL_0}, \tag{C5}$$

$$k_\pm = k_0 \pm \frac{t}{\sqrt{2LL_0}} \Rightarrow \omega_\pm = \omega_0 \pm \frac{ct}{\sqrt{2LL_0}}. \tag{C6}$$

The calculation confirms the possibility of generation of the closely separated symmetric mode triplet in the cavity. Since the frequency of the mechanical oscillator ω_m equals to the difference of the adjacent optical mode frequencies $\omega_+ - \omega_0 = \omega_0 - \omega_-$, we write

$$\omega_m = c\,\delta k = \frac{ct}{\sqrt{2LL_0}}. \tag{C7}$$

We check the dependence of the eigenfrequencies on the position x of the membrane to confirm the derivations made in Sec. V of the paper. In the general characteristic equation (C2) we set $L_1 = L + x$ and $L_2 = L - x$ ($x \ll L$) and get the following:

$$\begin{aligned} 1 - e^{4ikL}e^{2ikL_0} - 2re^{2ikL}(1 - e^{2ikL_0})\cos 2kx&\\ + r^2(e^{4ikL} - e^{2ikL_0}) = 0.& \end{aligned} \tag{C8}$$

Since $\cos 2kx \approx 1 + 2(kx)^2$, thus, in linear approximation the characteristic equation (C8) does not depend on the position x and turns into (C4). The eigenfrequencies also do not depend on the position of the membrane x.

2. The eigenmodes

To derive the eigenmode dependence on the membrane displacement x we use (1) equations that bound the fields in the different parts of the resonator, resulting from (C1),

$$tb = (e^{2ikL_1} - r)f,$$
$$tb = (1 - re^{2ikL_2})e^{-ikL_0}c; \tag{C9}$$

(2) the condition of small transmissivity $t \ll 1$,

$$r \approx 1 - \frac{t^2}{2}; \tag{C10}$$

(3) the condition that the thin membrane is in the middle of the long resonator,

$$L_1 = L + x, \quad L_2 = L - x, \quad \alpha \equiv \sqrt{\frac{L_0}{L}} \ll 1; \tag{C11}$$

and (4) equations for the eigenmodes' wave vectors (C6) in the limit $t^2 \ll \delta k\, L \ll 1$:

$$e^{2ik_0L_0} = e^{2ik_0L} = 1,$$
$$e^{2ik_\pm L_0} = 1 \pm \sqrt{2}it\sqrt{\frac{L_0}{L}} = 1 \pm \sqrt{2}i\alpha t,$$
$$e^{2ik_\pm L} = 1 \pm \sqrt{2}it\sqrt{\frac{L}{L_0}} = 1 \pm \sqrt{2}i\alpha^{-1}t. \tag{C12}$$

Substituting Eqs. (C10)–(C12) into (C9) we express the amplitude of the field in the membrane and the right part of the resonator via the amplitude of the field in the left part of the resonator for all of the modes: (1) k_+,

$$A_1 = f, A_0 = b = \left(\frac{\sqrt{2}i}{\alpha} - \frac{2ik_0x}{t}\right)f,$$
$$A_2 = \left(-1 + \frac{2\sqrt{2}\alpha k_0 x}{t}\right)f; \tag{C13}$$

(2) k_0,

$$A_1 = f,\ A_0 = b = \frac{t}{2} - \frac{2ik_0x}{t}f,\ A_2 = -\frac{2ik_0x}{t}f; \tag{C14}$$

and (3) k_-,

$$A_1 = f,\ A_0 = b = \left(-\frac{\sqrt{2}i}{\alpha} - \frac{2ik_0x}{t}\right)f,$$
$$A_2 = \left(-1 - \frac{2\sqrt{2}\alpha k_0 x}{t}\right)f. \tag{C15}$$

Using these expressions we can construct the *normalized* eigenmodes $[||\hat{v}_i|| = 1 + O(t^2) + O(x^2)]$:

$$\hat{v}_+^T = \left(\frac{\alpha}{\sqrt{2}} + \frac{\alpha^2 k_0 x}{t},\ i,\ -\frac{\alpha}{\sqrt{2}} + \frac{\alpha^2 k_0 x}{t}\right),$$
$$\hat{v}_0^T = \left(\frac{1}{\sqrt{2}},\ \frac{t}{2\sqrt{2}} - \frac{\sqrt{2}ik_0x}{t},\ \frac{1}{\sqrt{2}}\right), \tag{C16}$$
$$\hat{v}_-^T = \left(\frac{\alpha}{\sqrt{2}} - \frac{\alpha^2 k_0 x}{t},\ -i,\ -\frac{\alpha}{\sqrt{2}} - \frac{\alpha^2 k_0 x}{t}\right).$$

We can write the transformation matrix V from the partial modes A_2, A_0, and A_1 to the eigenmodes $\hat{v}_+$, $\hat{v}_0$, and $\hat{v}_-$:

$$V = \begin{pmatrix} \frac{\alpha}{\sqrt{2}} + \frac{\alpha^2 k_0 x}{t} & i & -\frac{\alpha}{\sqrt{2}} + \frac{\alpha^2 k_0 x}{t} \\ \frac{\sqrt{2}}{2} & \frac{t}{2} - \frac{\sqrt{2}ik_0x}{t} & \frac{\sqrt{2}}{2} \\ \frac{\alpha}{\sqrt{2}} - \frac{\alpha^2 k_0 x}{t} & -i & -\frac{\alpha}{\sqrt{2}} - \frac{\alpha^2 k_0 x}{t} \end{pmatrix}. \tag{C17}$$

Since these vectors are normalized, V is a unitary matrix and $V^{-1} = V^\dagger$. We introduce two more matrices: the unperturbed matrix V_0 and the matrix V_x, that contains the dependence on the displacement x:

$$V_0 \equiv V(x = 0) = \begin{pmatrix} \frac{\alpha}{\sqrt{2}} & i & -\frac{\alpha}{\sqrt{2}} \\ \frac{\sqrt{2}}{2} & \frac{t}{2} & \frac{\sqrt{2}}{2} \\ \frac{\alpha}{\sqrt{2}} & -i & -\frac{\alpha}{\sqrt{2}} \end{pmatrix}, \tag{C18}$$

$$V_x \equiv V - V_0 = \begin{pmatrix} \frac{\alpha^2 k_0 x}{t} & 0 & \frac{\alpha^2 k_0 x}{t} \\ 0 & -\frac{\sqrt{2}ik_0x}{t} & 0 \\ -\frac{\alpha^2 k_0 x}{t} & 0 & -\frac{\alpha^2 k_0 x}{t} \end{pmatrix}. \tag{C19}$$

Let

$$W = \begin{pmatrix} \omega_+ & 0 & 0 \\ 0 & \omega_0 & 0 \\ 0 & 0 & \omega_- \end{pmatrix}; \tag{C20}$$

then $\hat{u}^T = (A_2, A_0, A_1)$ is the vector of the partial modes and $\hat{v}^T = (\hat{v}_+, \hat{v}_0, \hat{v}_-)$ is the vector of the eigenmodes. We also introduce the vector $\hat{c}^T = \hat{v}^T(x = 0)$, which is unperturbed by the displacement x vector of the eigenmodes. They are bounded by the following relations:

$$\hat{v} = V\hat{u}, \quad \hat{c} = V_0\hat{u}. \tag{C21}$$

3. The interaction Hamiltonian

The Hamiltonian can be written in the following form:

$$\begin{aligned}\hat{H} &= \hat{v}^\dagger \hbar W \hat{v} = \hat{u}^\dagger C^\dagger \hbar W C \hat{u} \\ &= \hat{u}^\dagger (C_0^\dagger + C_x^\dagger)\hbar W (C_0 + C_x)\hat{u} \\ &= \hat{u}^\dagger C_0^\dagger (1 + C_0 C_x^\dagger)\hbar W (1 + C_x C_0^\dagger) C_0 \hat{u} \\ &= \hat{c}^\dagger (1 + C_0 C_x^\dagger)\hbar W (1 + C_x C_0^\dagger)\hat{c}.\end{aligned} \tag{C22}$$

We rewrite the Hamiltonian $\hat{H}$ and separate its parts describing the energy of the optical modes H_0 and the optomechanical interaction $\hat{H}_{\text{int}}$:

$$\begin{aligned}\hat{H} &= \hbar(\hat{c}_+^\dagger,\ \hat{c}_0^\dagger,\ \hat{c}_-^\dagger)\begin{pmatrix} \omega_+ & \frac{\alpha\omega_0 x}{L} & 0 \\ \frac{\alpha\omega_0 x}{L} & \omega_0 & \frac{\alpha\omega_0 x}{L} \\ 0 & \frac{\alpha\omega_0 x}{L} & \omega_- \end{pmatrix}\begin{pmatrix} \hat{c}_+ \\ \hat{c}_0 \\ \hat{c}_- \end{pmatrix} \\ &= \hat{H}_0 + \hat{H}_{\text{int}},\end{aligned} \tag{C23}$$

$$\hat{H}_0 \equiv \hbar\omega_+\hat{c}_+^\dagger\hat{c}_+ + \hbar\omega_0\hat{c}_0^\dagger\hat{c}_0 + \hbar\omega_-\hat{c}_-^\dagger\hat{c}_-, \tag{C24}$$

$$\hat{H}_{\rm int} \equiv \hbar\frac{\alpha\omega_0}{L}x(\hat{c}_0^\dagger\hat{c}_+ + \hat{c}_+^\dagger\hat{c}_0 + \hat{c}_-^\dagger\hat{c}_0 + \hat{c}_0^\dagger\hat{c}_-). \tag{C25}$$

Introducing slow amplitudes

$$x = x_0(de^{-i\omega_m t} + d^\dagger e^{i\omega_m t}), \tag{C26}$$

$$\hat{c}_0 = c_0 e^{-i\omega_0 t},\ \hat{c}_\pm = c_\pm e^{-i\omega_\pm t}, \tag{C27}$$

we omit the fast oscillating terms in the interaction Hamiltonian:

$$\hat{H}_{\rm int} = \hbar\omega_0\frac{\alpha x_0}{L}[c_0(dc_+^\dagger + d^\dagger c_-^\dagger) + c_0^\dagger(d^\dagger c_+ + dc_-)], \tag{C28}$$

a result that coincides with (2.2b) and (5.4) at substitution $c_0 \to -ic_0,\ c_0^\dagger \to ic_0^\dagger$ ($\pi/2$ phase shift).

APPENDIX D: DERIVATION OF THE HAMILTONIAN FOR THE TWO-MODE SCHEME

We start from calculation of the light pressure force acting on a movable mirror M shown in Fig. 5. Phase shifts resulting from the beam splitter and mirror M are practically the same for the modes $\omega_\pm$, and ω_0, i.e., distances $L_{1,2}$ in Fig. 5 are much smaller than $\ell_{1,2}$. We also assume that frequencies $\omega_\pm$ and ω_0 are close to each other (i.e., $\ell_1 \simeq \ell_2$), so calculating the ponderomotive force we denote $\omega_- \simeq \omega_+ = \tilde{\omega}$ as well as $\ell_1 \simeq \ell_2 = \tilde{\ell}$.

The resultant ponderomotive force is equal to the difference of forces acting from the left and top and from the right and bottom:

$$F_{lp} = \frac{\hbar\tilde{\omega}}{\tilde{\ell}}\left(\frac{\hat{c}_+^\dagger + \hat{c}_-^\dagger}{\sqrt{2}}\frac{\hat{c}_+ + \hat{c}_-}{\sqrt{2}} - \frac{\hat{c}_+^\dagger - \hat{c}_-^\dagger}{\sqrt{2}}\frac{\hat{c}_+ - \hat{c}_-}{\sqrt{2}}\right) = \frac{\hbar\tilde{\omega}}{\tilde{\ell}}(\hat{c}_+^\dagger\hat{c}_- + \hat{c}_-^\dagger\hat{c}_+). \tag{D1}$$

Here $\hat{c}_\pm$ are amplitudes of modes $\omega_\pm$ on the beam splitter surface. The *direct* terms ($\hat{c}_+^\dagger\hat{c}_+$ and $\hat{c}_-^\dagger\hat{c}_-$) are absent and only *cross* terms ($\hat{c}_+^\dagger\hat{c}_-$ and $\hat{c}_-^\dagger\hat{c}_+$) survive. In the linear approximation light pressure force is

$$F_{lp} \simeq \frac{\hbar\tilde{\omega}}{\tilde{\ell}}(C_{0+}^*\hat{c}_- + C_{0+}\hat{c}_-^\dagger + C_{0-}^*\hat{c}_+ + C_{0-}\hat{c}_+^\dagger). \tag{D2}$$

Here $C_{0\pm}$ are mean amplitudes at the beam splitter created by the pump with frequency ω_0. Using (2.3) we present the interaction Hamiltonian in the form

$$H_{\rm int} = -F_{lp}x_0(\hat{d} + \hat{d}^\dagger). \tag{D3}$$

Keeping in mind condition (2.1) and time dependences

$$\hat{c}_\pm \sim e^{-i\omega_\pm t},\quad \hat{c}_\pm^\dagger \sim e^{i\omega_\pm t},\quad C_{0\pm} \sim e^{-i\omega_0 t} \tag{D4}$$

we omit fast oscillating terms in the Hamiltonian and keep slow terms only:

$$H_{\rm int} = -\frac{\hbar\tilde{\omega}x_0}{\tilde{\ell}}(\hat{d}[C_{0+}^*\hat{c}_- + C_{0-}\hat{c}_+^\dagger] \tag{D5}$$

$$+ \hat{d}^\dagger[C_{0+}\hat{c}_-^\dagger + C_{0-}^*\hat{c}_+]). \tag{D6}$$

Choosing

$$C_{0-} = i|C|,\quad C_{+0} = -i|C| \tag{D7}$$

we finally get formula (5.4), which is similar to (2.2b).

[1] B. P. Abbott *et al.* (LVC Collaboration), Prospects for observing and localizing gravitational-wave transients with advanced LIGO, advanced virgo and KAGRA, Living Rev Relativ **23**, 3 (2020).

[2] J. Aasi, J Abadie, B. P. Abbott *et al.*, Characterization of the LIGO detectors during their sixth science run, Classical Quantum Gravity **32**, 115012 (2015).

[3] D. Martynov *et al.*, Sensitivity of the advanced LIGO detectors at the beginning of gravitational wave astronomy, Phys. Rev. D **93**, 112004 (2016).

[4] F. Asernese *et al.*, Advanced Virgo: A 2nd generation interferometric gravitational wave detector, Classical Quantum Gravity **32**, 024001 (2015).

[5] K. L. Dooley, J. R. Leong, T. Adams, C. Affeldt, A. Bisht, C. Bogan, J. Degallaix, C. Graf, S. Hild, and J. Hough, GEO 600 and the GEO-HF upgrade program: Successes and challenges, Classical Quantum Gravity **33**, 075009 (2016).

[6] Y. Aso, Y. Michimura, K. Somiya, M. Ando, O. Miyakawa, T. Sekiguchi, D. Tatsumi, and H. Yamamoto, Interferometer design of the KAGRA gravitational wave detector, Phys. Rev. D **88**, 043007 (2013).

[7] S. Forstner, S. Prams, J. Knittel, E. D. van Ooijen, J. D. Swaim, G. I. Harris, A. Szorkovszky, W. P. Bowen, and H. Rubinsztein-Dunlop, Cavity Optomechanical Magnetometer, Phys. Rev. Lett. **108**, 120801 (2012).

[8] B.-B. Li, J. Bílek, U. Hoff, L. Madsen, S. Forstner, V. Prakash, C. Schafermeier, T. Gehring, W. Bowen, and U. Andersen, Quantum enhanced optomechanical magnetometry, Optica **5**, 850 (2018).

[9] M. Wu, A. C. Hryciw, C. Healey, D. P. Lake, H. Jayakumar, M. R. Freeman, J. P. Davis, and P. E. Barclay, Dissipative and Dispersive Optomechanics in a Nanocavity Torque Sensor, Phys. Rev. X **4**, 021052 (2014).

[10] P. H. Kim, B. D. Hauer, C. Doolin, F. Souris, and J. P. Davis, Approaching the standard quantum limit of mechanical torque sensing, Nat. Commun. **7**, 13165 (2016).

[11] J. Ahn, Z. Xu, J. Bang, P. Ju, X. Gao, and T. Li, Ultrasensitive torque detection with an optically levitated nanorotor, Nat. Nanotechnol. **15**, 89 (2020).

[12] V. B. Braginskii, Classical and quantum restrictions on the detection of weak disturbances of a macroscopic oscillator, JETP **26**, 831 (1968).

[13] V. B. Braginsky and F. Ya. Khalili, *Quantum Measurement* (Cambridge University, New York, 1992).

[14] V. B. Braginsky and F. Ya. Khalili, Gravitational wave antenna with QND speed meter, Phys. Lett. A **147**, 251 (1990).

[15] V. B. Braginsky, M. L. Gorodetsky, F. Y. Khalili, and K. S. Thorne, Dual-resonator speed meter for a free test mass, Phys. Rev. D **61**, 044002 (2000).

[16] V. B. Braginsky and F. Ya. Khalili, Low noise rigidity in quantum measurements, Phys. Lett. A **257**, 241 (1999).
[17] F. Ya. Khalili, Frequency-dependent rigidity in large-scale interferometric gravitational-wave detectors, Phys. Lett. A **288**, 251 (2001).
[18] The LIGO Scientific collaboration, A gravitational wave observatory operating beyond the quantum shot-noise limit, Nat. Phys. **7**, 962 (2011).
[19] LIGO Scientific Collaboration and Virgo Collaboration, Enhanced sensitivity of the LIGO gravitational wave detector by using squeezed states of light, Nat. Photonics **7**, 613 (2013).
[20] V. Tse *et al.*, Quantum-Enhanced Advanced LIGO Detectors in the Era of Gravitational-Wave Astronomy, Phys. Rev. Lett. **123**, 231107 (2019).
[21] F. Asernese *et al.* (Virgo Collaboration), Increasing the Astrophysical Reach of the Advanced Virgo Detector via the Application of Squeezed Vacuum States of Light, Phys. Rev. Lett. **123**, 231108 (2019).
[22] M. Yap, J. Cripe, G. Mansell *et al.*, Broadband reduction of quantum radiation pressure noise via squeezed light injection, Nat. Photonics **14**, 19 (2020).
[23] H. Yu, L. McCuller, M. Tse *et al.*, Quantum correlations between light and the kilogram-mass mirrors of LIGO, Nature (London) **583**, 43 (2020).
[24] J. Cripe, N. Aggarwal, R. Lanza *et al.*, Measurement of quantum back action in the audio band at room temperature, Nature (London) **568**, 364 (2019).
[25] S. P. Vyatchanin and A. B. Matsko, Quantum limit on force measurements, JETP **77**, 218 (1993).
[26] S. Vyatchanin and E. Zubova, Quantum variation measurement of force, Phys. Lett. A **201**, 269 (1995).
[27] H. J. Kimble, Y. Levin, A. B. Matsko, K. S. Thorne, and S. P. Vyatchanin, Conversion of conventional gravitational-wave interferometers into QND interferometers by modifying input and/or output optics, Phys. Rev. D **65**, 022002 (2001).
[28] M. Tsang and C. M. Caves, Coherent Quantum-Noise Cancellation for Optomechanical Sensors, Phys. Rev. Lett. **105**, 123601 (2010).
[29] E. Polzik and K. Hammerer, Trajectories without quantum uncertainties, Ann. Phys. (NY) **527**, A15 (2014).
[30] C. Moller, R. Thomas, G. Vasilakis, E. Zeuthen, Y. Tsaturyan, M. Balabas, K. Jensen, A. Schliesser, K. Hammerer, and E. Polzik, Quantum back-action-evading measurement of motion in a negative mass reference frame, Nature (London) **547**, 191 (2017).
[31] A. B. Matsko, V. V. Kozlov, and M. O. Scully, Backaction Cancellation in Quantum Nondemolition Measurement of Optical Solitons, Phys. Rev. Lett. **82**, 3244 (1999).
[32] M. L. Povinelli, M. Lončar, M. Ibanescu, E. J. Smythe, S. G. Johnson, F. Capasso, and J. D. Joannopoulos, Evanescent-wave bonding between optical waveguides, Opt. Lett. **30**, 3042 (2005).
[33] A. V. Maslov, V. N. Astratov, and M. I. Bakunov, Resonant propulsion of a microparticle by a surface wave, Phys. Rev. A **87**, 053848 (2013).
[34] S. P. Vyatchanin, A. I. Nazmiev, and A. B. Matsko, Broadband dichromatic variational measurement, Phys. Rev. A **104**, 023519 (2021).
[35] V. Braginsky, Y. Vorontsov, and K. Thorne, Quantum nondemolition measurements, Science **209**, 547 (1980).
[36] V. Braginsky, Yu. I. Vorontsov, and F. Y. Khalili, Optimal quantum measurements in detectors of gravitation radiation, JETP Lett. **27**, 296 (1978).
[37] K. Thorne, R. Drever, C. Caves, M. Zimmermann, and V. Sandberg, Quantum Nondemolition Measurements of Harmonic Oscillators, Phys. Rev. Lett. **40**, 667 (1978).
[38] A. Clerk, F. Marquardt, and K. Jacobs, Back-action evasion and squeezing of a mechanical resonator using a cavity detector, New J. Phys. **10**, 095010 (2008).
[39] S. Vyatchanin and A. Matsko, On sensitivity limitations of a dichromatic optical detection of a classical mechanical force, J. Opt. Soc. Am. B **35**, 1970 (2018).
[40] M. Tsang and C. M. Caves, Evading Quantum Mechanics: Engineering a Classical Subsystem within a Quantum Environment, Phys. Rev. X **2**, 031016 (2012).
[41] X. Li, M. Korobko, Y. Ma, R. Schnabel, and Y. Chen, Coherent coupling completing an unambiguous optomechanical classification framework, Phys. Rev. A **100**, 053855 (2019).
[42] A. Nazmiev, A. Matsko, and S. P. Vyatchanin, Back action evading electro-optical transducer, J. Opt. Soc. Am. B **39**, 1103 (2022).
[43] C. F. Ockeloen-Korppi, E. Damskagg, J. M. Pirkkalainen, A. A. Clerk, M. J. Woolley, and M. A. Sillanpaa, Quantum Backaction Evading Measurement of Collective Mechanical Modes, Phys. Rev. Lett. **117**, 140401 (2016).
[44] D. Walls and G. Milburn, *Quantum Optics* (Springer-Verlag, Berlin, 2008).